

1
2 **Insight into the Composition of Organic Compounds**
3 **($\geq C_6$) in PM_{2.5} in Wintertime in Beijing, China**
4

5 **Ruihe Lyu^{1,2}, Zongbo Shi², Mohammed Salim Alam²,**
6 **Xuefang Wu^{2,4}, Di Liu², Tuan V. Vu², Christopher Stark²,**
7 **Pingqing Fu³, Yinchang Feng¹ and Roy M. Harrison^{2†*}**
8

9 ¹ **State Environmental Protection Key Laboratory of Urban Ambient Air**
10 **Particulate Matter Pollution Prevention and Control, College of**
11 **Environmental Science and Engineering**
12 **Nankai University, Tianjin 300350, China**
13

14 ² **Division of Environmental Health and Risk Management**
15 **School of Geography, Earth and Environmental Sciences, University of**
16 **Birmingham Edgbaston, Birmingham B15 2TT, UK**
17

18 ³ **Institute of Surface Earth System Science, Tianjin University**
19 **Tianjin, 300350, China**
20

21 ⁴ **Regional Department of Geology and Mineral Resources, China**
22 **University of Geosciences, Xueyuan Road 29, 100083 Beijing China**
23

24
25 **† Also at: Department of Environmental Sciences / Centre of Excellence in**
26 **Environmental Studies, King Abdulaziz University, PO Box 80203, Jeddah, 21589,**
27 **Saudi Arabia**
28

29
30 **Corresponding author: E-mail: r.m.harrison@bham.ac.uk (Roy M. Harrison)**
31

32 **ABSTRACT**

33 Organic matter is a major component of PM_{2.5} in megacities. In order to understand the detailed
34 characteristics of organic compounds ($\geq C_6$) at a molecular level on non-haze and haze days, we
35 determined more than 300 organic compounds in the PM_{2.5} from an urban area of Beijing collected in
36 November-December 2016 using two-dimensional gas chromatography coupled to time-of-flight mass
37 spectrometry (GC \times GC-TOFMS). The identified organic compounds have been classified into groups,
38 and quantitative methods were used to calculate their concentrations. Primary emission sources make
39 significant contributions to the atmospheric organic compounds and six groups (including n-alkanes,
40 polycyclic aromatic hydrocarbons (PAHs), levoglucosan, branched-alkanes, n-alkenes and alkyl-
41 benzenes) account for 66% of total identified organic compound mass. In addition, PAHs, and
42 oxygenated PAHs (O-PAHs) were abundant amongst the atmospheric organic compounds on both haze
43 and non-haze days. The most abundant hydrocarbon groups were observed with a carbon atom range of
44 C₁₉-C₂₈. In addition, the total concentration of unidentified compounds present in the chromatogram was
45 estimated in the present study. The total identified compounds account for approximately 47% of total
46 organic compounds ($\geq C_6$) in the chromatogram on both the non-haze and haze days. The total mass
47 concentrations of organic compounds ($\geq C_6$) in the chromatogram were 4.0 $\mu\text{g m}^{-3}$ and 7.4 $\mu\text{g m}^{-3}$ on the
48 non-haze and haze days respectively, accounting for 26.4% and 18.5% of organic matter respectively on
49 those days estimated from the total organic carbon concentration. Ratios of individual compound
50 concentrations between haze and non-haze days do not give a clear indication of the degree of oxidation,
51 but the overall distribution of organic compounds in the chromatogram provides strong evidence that the
52 organic aerosol is less G.C.-volatile and hence more highly oxidised on haze days.

53

54 **Keywords:** Organic aerosol; GC \times GC-TOFMS; PAHs; Haze; PM_{2.5} Beijing, China

55

56 **1. INTRODUCTION**

57 China is suffering from severe PM_{2.5} pollution, especially in its capital, the annual average concentration
58 of PM_{2.5} in Beijing being in the range 69.7~122 µg m⁻³ from 2000 to 2015 (Lang et al., 2017), 2.0~3.5
59 times the national standard (35 µg m⁻³). A recent study showed that the average PM_{2.5} concentration
60 during the haze days was 256 µg m⁻³ in the winter period from December 1, 2015 to December 31, 2015
61 in Beijing, and very much higher than that of non-haze days (24.7 µg m⁻³) (Li, et al. 2019), and 25 times
62 the World Health Organization (WHO) guideline of 10 µg m⁻³.

63
64 Organic matter is a large and important fraction of atmospheric fine particles, and a substantial number
65 of organic compounds can be found in the atmospheric particulate phase and may originate as either
66 primary emissions or from secondary formation process (Wu et al., 2018). The primary emission tracers
67 and precursor compounds have been extensively studied in the Beijing aerosol and showed significant
68 contributions from coal combustion, biomass burning and traffic emissions (Ren et al., 2016; Yao et al.,
69 2016). These studies concentrated on the identification of individual organic compounds from the organic
70 aerosol, such as n-alkanes, n-alkenes, PAHs and hopanes, but the structurally specific identification of
71 the chemical composition of the organic aerosol is far from complete. Due to its huge complexity,
72 particulate organic matter is still inadequately characterized up to the present. Hence, the identification
73 of organic compounds in generic groups may be more informative in elucidating the molecular
74 distribution of atmospheric organic compounds, and bulk aerosol characteristics (Alam et al., 2018).
75 Previous studies have shown that the organic compounds were highly oxidized during haze days, and
76 secondary formation has made a significant contribution to the PM (Li et al., 2019). However, these
77 studies focused only on specific individual oxidized organic compounds or the ratios of C, N and O to
78 assess the entire aerosol ageing process (Li et al., 2019), and the relationship between the molecular
79 distribution and oxidizing processes during haze formation is still not clear.

80

81 Two-dimensional gas chromatography (GC×GC) coupled with TOF-MS offers much enhanced
82 resolution of complex mixtures, and the technique has been extended in the last 10 years to encompass
83 atmospheric analysis. The two independent analytical dimensions in GC×GC-TOF/MS make this
84 technique potentially ideal for measuring the organic components within a complex matrix such as
85 ambient particulate matter (Hamilton et al., 2004; Welthagen et al., 2003), and its ability to separate
86 complex mixtures of organics at low concentrations makes it an ideal technique to measure partially
87 oxidised, isomeric and homologous series compounds and even groups of compounds (Alam et al., 2016a;
88 Alam and Harrison, 2016; Hamilton et al., 2004). In an earlier study of organic compounds in the Beijing
89 atmosphere, Zhou et al. (2009) reported that 68.4% of particulate organic matter was in the previously
90 “unresolved complex mixture” found in conventional GC separations. The GC × GC technique is able to
91 resolve and identify the components contributing to the unresolved mixture, and the molecular
92 distribution of atmospheric organic compounds can be clearly identified in the chromatogram.

93

94 In order to establish relationships between organic compounds in fine particles and their characteristics
95 on non-haze and haze days, as well as to identify the relative importance of their emission sources, further
96 investigation of particulate organic matter composition has been conducted. The objective of this study
97 was to investigate the organic compounds with carbon number higher than C₆ in PM_{2.5} samples collected
98 in central Beijing during wintertime, 2016. In this paper, particle samples were analysed by the GC×GC-
99 TOFMS technique after solvent extraction and the detailed organic composition was observed for polar
100 and non-polar organic compound groups. Here, we report a large number of organic compounds, and
101 their concentrations and molecular distributions sampled on non-haze and haze days. The characteristics
102 of the molecular distribution of atmospheric organic compounds on non-haze days were analysed and
103 compared with haze days during aerosol ageing. In addition, we report their possible sources, formation
104 processes, and reveal and assess their pollution characteristics during non-haze and haze periods. Finally,

105 the mass of unidentified organic compounds ($>C_6$) is estimated and compared between non-haze and
106 haze days.

107

108 **2. MATERIALS AND METHODS**

109 **2.1 Sampling Method and Site Characteristics**

110 $PM_{2.5}$ samples were collected at the Institute of Atmospheric Physics (IAP), Chinese Academy of
111 Sciences in Beijing, China. The sampling site ($39^{\circ}58'N$, $116^{\circ}22'E$) was located between the North 3rd
112 Ring Road and North 4th Ring Road. The site is approximately 1 km from the 3rd Ring Road, 200 m
113 west of the G6 Highway (which runs north-south) and 50 m south of Beitucheng West Road (which runs
114 east-west). The annual average vehicular speeds in the morning and evening traffic peak were 27.4 and
115 24.3 km h^{-1} , respectively. No industrial sources were located in the vicinity of the sampling site. The
116 experimental campaign took place from November 9 to December 11, 2016. The samples were collected
117 onto pre-baked quartz fibre filters (Pallflex) by a gravimetric high volume sampler (Tisch, USA) with a
118 $PM_{2.5}$ inlet at a flow rate of $1.0\text{ m}^3\text{ min}^{-1}$ during the sampling period. The collecting time was 24 h per
119 sample and 3 blank samples were collected during this period. The filters were previously enveloped
120 with aluminium foils and then baked at $450\text{ }^{\circ}C$ for 6 hours before sampling. After sampling, each filter
121 was packed separately and stored in a refrigerator below $-20^{\circ}C$ until the analysis.

122

123 **2.2 Analytical Instrumentation**

124 The sample extracts were analyzed using a 2D gas chromatograph (GC, 7890A, Agilent Technologies,
125 Wilmington, DE, USA) equipped with a Zoex ZX2 cryogenic modulator (Houston, TX, USA). The first
126 dimension was separated on a SGE DBX5, non-polar capillary column (30.0 m, 0.25 mm ID, 0.25 mm
127 – 5.00% phenyl polysilphenylene-siloxane), and the second-dimension column was a SGE DBX50 (4.0
128 m, 0.10 mm ID, 0.10 mm – 50.0% phenyl polysilphenylene-siloxane). The GC \times GC was interfaced

129 with a Bench-ToF-Select, time-of-flight mass spectrometer (ToF-MS, Markes International, Llantrisant,
130 UK). The acquisition speed was 50.0 Hz with a mass resolution of >1200 fwhm at 70.0 eV and the mass
131 range was 35.0 to 600 m/z. All data produced were processed using GC Image v2.5 (Zoex Corporation,
132 Houston, US).

133

134 **2.3 Extraction and Analysis Methods of Filters**

135 The filters were spiked with 30.0 μL of 30.0 $\mu\text{g mL}^{-1}$ deuterated internal standards (pentadecane- d_{32} ,
136 eicosane- d_{42} , pentacosane- d_{52} , triacontane- d_{62} , butylbenzene- d_{14} , nonylbenzene-2,3,4,5,6- d_5 , biphenyl-
137 d_{10} , p-terphenyl- d_{14} ; Sigma-Aldrich, UK) for quantification and then immersed in
138 methanol/dichloromethane (DCM) (1:1, v/v), and ultra-sonicated for 20 min at 20°C. The extract was
139 filtered using a clean glass pipette column packed with glass wool and anhydrous Na_2SO_4 , and
140 concentrated to 100 μL under a gentle flow of nitrogen for analysis using GC \times GC-ToF-MS. 1 μL of
141 the extracted sample was injected in a split ratio 50:1 at 300°C. The initial temperature of the primary
142 oven (80°C) was held for 2 min and then increased at 2°C min^{-1} to 210°C, followed by 1.5 °C min^{-1} to
143 325°C. The initial temperature of the secondary oven (120°C) was held for 2 min and then increased at
144 3°C min^{-1} to 200°C, followed by 2°C min^{-1} to 300°C and a final increase of 1°C min^{-1} to 330°C to ensure
145 all species passed through the column. The transfer line temperature was 330°C and the ion source
146 temperature was 280°C. Helium (99.999%) was used as the carrier gas at a constant flow rate of 1 mL
147 min^{-1} . Further details of the instrumentation and data processing methods are given by Alam and
148 Harrison (2016) and Alam et al. (2016a).

149

150 **2.4 Qualitative and Quantitative Analysis**

151 Standards used in these experiments included 26 n-alkanes (C_{11} to C_{36}), EPA's 16 priority pollutant
152 PAHs, 4 hopanes (17 α (H),21 β (H)-22R-homohopane, 17 α (H),21 β (H)-hopane, 17b(H),21a(H)-30-

153 norhopane and 17 α (H)-22,29,30-trisnorhopane, 7 decalins and tetralines (cis/trans-decalin, tetralin, 5-
154 methyltetraline, 2,2,5,7-tetramethyltetraline, 2,5,8-trimethyltetraline and 1,4-dimethyltetraline), 4
155 alkyl-naphthalenes (1-methyl-naphthalene, 1-ethyl-naphthalene, 1-n-propyl-naphthalene and 1-n-
156 hexyl-naphthalene), 13 alkyl-cyclohexanes (n-heptyl-cyclohexane to n-nonadecyl-cyclohexane), 5
157 alkyl-benzenes (n-butyl-benzene, n-hexyl-benzene, n-octyl-benzene, n-decyl-benzene and n-dodecyl-
158 benzene) (Sigma-Aldrich, UK, purity >99.2%), 11 n-aldehydes (C₈ to C₁₃) (Sigma-Aldrich, UK, purity
159 \geq 95.0%), C₁₄ to C₁₈ (Tokyo Chemical Industry UK Ltd, purity >95.0%); and 11 2-ketones, C₈ to C₁₃
160 and C₁₅ to C₁₈ (Sigma-Aldrich, UK, purity \geq 98.0%) and C₁₄ (Tokyo Chemical Industry UK Ltd, purity
161 97.0%), 4 n-alcohols (2-decanol, 2-dodecanol, 2-hexadecanol and 2-nonadecanol) (Sigma-Aldrich, UK,
162 purity 99.0%) and 1-pentadecanol (Sigma-Aldrich, UK, purity 99.0%).

163

164 Compound identification was based on the GC \times GC-TOFMS spectral library, NIST mass spectral
165 library and on co-injection with authentic standards. Compounds within the homologous series for
166 which standards were not available were identified by comparing the retention time interval between
167 homologues, and by comparison of mass spectra with the standards for similar compounds within the
168 series, by comparison to the NIST mass spectral library, and by the analysis of fragmentation patterns.
169 The quantification for identified compounds was performed by the linear regression method using the
170 seven-point calibration curves (0.05, 0.10, 0.25, 0.50, 1.00, 2.00, 3.00 ng μ L⁻¹) established between the
171 authentic standards/internal standard concentration ratios and the corresponding peak area ratios. The
172 calibration curves for all target compounds were highly linear ($r^2 > 0.98$, from 0.978 to 0.998),
173 demonstrating the consistency and reproducibility of this method. Limits of detection for individual
174 compounds were typically in the range 0.001–0.08 ng m⁻³. The identified compounds which have no
175 commercial authentic standards were quantified using the calibration curves for similar structure
176 compounds or isomeric compounds. This applicability of quantification of individual compounds using

177 isomers of the same compound functionality (which have authentic standards) has been discussed
178 elsewhere and has a reported uncertainty of 24% (Alam et al., 2018).

179

180 The branched alkanes, alkyl-benzenes, alkyl-decalins, alkyl-phenanthrene and anthracene (alkyl-Phe and
181 Ant), alkyl-naphthalene (alkyl-Nap) and alkyl-benzaldehyde were identified in the samples with the
182 graphics method of the GC Image v2.5 (Zoex Corporation, Houston, US), and the detailed descriptions
183 are given elsewhere (Alam et al., 2018). Briefly, the structurally similar compounds (similar physico-
184 chemical properties) were identified as a group via drawing a polygon around a section of the
185 chromatogram with the polygon selection tool. All compounds included in the polygon belong to a
186 special compound class and the total concentrations were calculated via a calibration curve of the
187 adjacent compounds and internal standards (IS).

188

189 Field and laboratory blanks were routinely analysed to evaluate analytical bias and precision. Blank
190 levels of individual analytes were normally very low and, in most cases, not detectable. The major
191 contaminants observed were very minor amounts of n-alkanes ranging from C₁₁ to C₂₁, with no carbon
192 number predominance and maximum at C₁₈; PAH were not detectable. The major proportion of the
193 contaminants could be distinguished by their low concentrations and distribution fingerprints (especially
194 the n-alkanes). These contaminants did not interfere with the recognition or quantification of the
195 compounds of interest. Recovery efficiencies were determined by analysing the blank samples spiked
196 with standard compounds. Mean recoveries ranged between 82 and 98%. All quantities reported here
197 have been corrected according to their recovery efficiencies. Analytical data from the GC×GC analysis
198 were compared with a conventional GC-MS analysis for levoglucosan and 13 PAH. The results from two
199 analytical instruments were compared, and the correlations (r^2) between them were in the range of 0.5 to
200 0.8 with 10 mean concentrations of individual compounds from each technique within 20% of one

201 another, 2 within 20-30% and the remainder (2) within 30-40% of one another. The largest outlier was
202 levoglucosan, which was underestimated, probably since it decomposed due to a lack of the usual
203 derivatisation.

204

205 **3. RESULTS AND DISCUSSION**

206 **3.1 General Aerosol Characteristics**

207 Thirty-three samples were separated into non-haze (13) and haze (20) days (the latter with PM_{2.5}
208 exceeding 75 µg m⁻³ for 24 h average) according to the National Ambient Air Quality Standards of China
209 (NAAQS) released in 2012 by the Ministry of Environmental Protection (MEP) of the People's Republic
210 of China. The concentrations of PM_{2.5}, black carbon (BC), organic carbon (OC), element carbon (EC),
211 gaseous pollutants (SO₂, NO, NO₂, NO_x, and CO) and meteorological parameters (wind speed (WS),
212 wind direction (WD) and relative humidity (RH)) were simultaneously determined during the field
213 campaigns and appear in Table S1.

214

215 The average daily PM_{2.5} mass was 99 µg m⁻³, and haze days (average 141 µg m⁻³) were four times higher
216 than that of non-haze days (35.3 µg m⁻³). The wind and temperature during the haze and non-haze days
217 were 0.94 and 1.44 m/s, 6.07 and 4.0°C, respectively. However, the relative humidity during haze
218 episodes (56.3%) was slightly higher than the non-haze periods (39.8%). The concentrations of gaseous
219 pollutants SO_x, NO_x, and CO were simultaneously elevated with the increase of PM_{2.5} concentrations,
220 whereas the O₃ concentration presented an opposite trend to PM_{2.5} concentrations (Lyu et al., 2019). The
221 average concentration of organic matter (OM) was estimated as 30.2 µg m⁻³ using the OC concentration
222 (18.9 µg m⁻³) and a multiplying factor of 1.6 for aged aerosols (Turpin and Lim, 2001). The OM
223 concentration was 40.0 µg m⁻³ and 15.0 µg m⁻³ on haze and non-haze days respectively.

224

225 3.2 The Major Classes of Organic Compounds in PM_{2.5}

226 More than 6000 peaks were found in the 2D chromatogram image of each sample by the data processing
227 software (GC Image v2.5). Over 300 polar and non-polar organic compounds (POCs and N-POCs) were
228 identified and quantified in the PM_{2.5} samples, and these compounds are grouped into more than twenty
229 classes, including normal and branched alkanes, n-alkenes, aliphatic carbonyl compounds (1-alkanals, n-
230 alkan-2-ones and n-alkan-3-ones), n-alkanoic acids, n-alkanols, PAHs, oxygenated PAHs (OPAHs),
231 alkylated-PAHs, hopanes, alkyls-benzenes, alkyl-cyclohexanes, pyridines, quinolines, furanones, and
232 biomarkers (levoglucosan, cedrol, phytane, pristane, supraene and phytone). The details of aliphatic
233 hydrocarbon measurements (including n-alkanes, n-alkenes) and carbonyl compounds (including n-
234 alkanals, n-alkan-2-ones, n-alkan-3-ones, furanones and phytone) have been reported in previous articles
235 (Lyu et al. 2018a,b). The total concentrations of identified organic compounds ranged from 0.94 to 5.14
236 $\mu\text{g m}^{-3}$ with the average of $2.84 \pm 1.19 \mu\text{g m}^{-3}$, accounting for 9.40 % of OM. The concentrations of
237 identified individual organic compounds are summarized in Table S2, and the percentage of each group
238 in the total identified organic compounds is in Figure 1. The n-alkanes (16%) make the greatest
239 contribution to the total mass of identified organic compounds, followed by levoglucosan (13%),
240 branched-alkanes (13%), PAHs (10%), n-alkenes (7%) and alkyl-benzenes (7%). These six groups
241 account for 66% of total identified organic compounds by mass, and a total concentration of $1.41 \mu\text{g m}^{-3}$,
242 accounting for 1.42% of the particle mass. In a study in Nanjing, Haque et al. (2019) reported the most
243 abundant classes of organic compounds to be n-alkanes (205 ng m^{-3}), followed by fatty acids (76.3 ng m^{-3}),
244 PAHs (64.3 ng m^{-3}), anhydrosugars (levoglucosan, galactosan and mannosan, 56.3 ng m^{-3}), fatty
245 alcohols (40.5 ng m^{-3}) and phthalate esters (15.2 ng m^{-3}).

246

247 **3.3 The Characteristics of Organic Compound Groups on Non-haze and Haze Days**

248 The average total concentration of identified groups was calculated for the non-haze (13 days) and haze
249 periods (20 days). The comparisons of two periods (non-haze and haze days) are shown in Figure 2, and
250 the detailed concentrations of each group are shown in the Table S3. The concentrations of most organic
251 compound groups on the haze days were higher than non-haze days, especially for the n-alkanols and n-
252 C_n-cyclohexanes. The alkyl-benzenes, alkyl-benzaldehydes, monoaromatic compounds and quinoline
253 have approximately similar concentrations on the non-haze and haze days.

254

255 As many compound groups have not been reported in previous studies, and complete data on the relative
256 abundance of these compounds in various source emissions are not available at present, it is not yet
257 possible to calculate source contributions to ambient organic compound concentrations via molecular
258 marker or mathematical modelling methods. However, several important consistency checks on the
259 potential source can be performed. In the sections that follow, the literature on the origin of each of these
260 compound classes is reviewed briefly and the measured compound concentrations are described. Table
261 1 shows the comparison of identified organic compounds between the present and previous studies in
262 Beijing. In many, but not all cases, concentrations are comparable.

263

264 **3.3.1 n-Alkanoic acids, n-alkanols and carbonyl compounds**

265 The n-alkanoic acids with carbon numbers from C₆ to C₁₀ were identified in the PM_{2.5}. Higher molecular
266 weight alkanolic acids generated from the biomass burning (Simoneit and Mazurek, 1982) were not
267 identified from the samples probably due to low volatility in the G.C. The n-alkanoic acids were
268 observed at a similar magnitude to a previous study in Beijing (Zhou et al., 2009) (Table 1).

269

270 Previous studies have found that the n-alkanoic acid homologues were significantly impacted by cooking

271 emissions in Beijing and showed higher concentrations on non-haze days and a similar distribution
272 pattern in all seasons (Huang et al., 2006; He et al., 2006b; Sun et al. 2013). Consistent results for acids
273 were observed in this study, and the Σ n-alkanoic acids had an average concentration on the non-haze
274 days with an average concentration of 36.4 ng m^{-3} , higher than 24.6 ng m^{-3} on haze days, strongly
275 implying a dominant contribution from cooking emissions as opposed to secondary formation.

276

277 In the present study, 1-alkanols with even-carbon numbers from C_{12} to C_{20} were identified in the $PM_{2.5}$,
278 with a quite similar molecular distribution to that of diesel engine exhaust samples (Alam et al., 2016b).
279 In addition, other primary emission sources may make a potential contribution to these compounds,
280 including from biomass burning (Zhang et al., 2007). The average Σ n-alkanols concentration was 38.5
281 ng m^{-3} , and Σ n-alkanols had higher concentrations on the haze days (59.8 ng m^{-3}), approximately eight
282 times greater than 8.39 ng m^{-3} on non-haze days. The above results suggest that n-alkanol formation is
283 more efficient on haze days, even though vehicular emissions appear to be another important source.

284

285 Aliphatic carbonyl compounds including n-alkanals, n-alkan-2-ones and n-alkan-3-ones, have been
286 described in detail by Lyu et al. (2019). Briefly, the daily sum of aliphatic carbonyls (Σ AC), ranged from
287 8.87 to 164 ng m^{-3} , accounting for 0.02 – 0.46% of OM. The average Σ AC was 75.8 ng m^{-3} during all
288 haze days, approximately double the 39.5 ng m^{-3} of the non-haze period. Lyu et al. (2019) showed that
289 the n-alkanals were mainly originated from vehicle exhaust or formed from OH oxidation of n-alkanes,
290 while the n-alkanones were probably emitted mainly by coal combustion.

291

292 **3.3.2 Nitrogen-containing organic compounds (N-CC)**

293 Nitrogen-containing (N-containing) organic compounds have been reported in many previous studies,
294 and the important sources of N-containing compounds are coal combustion, biomass burning, vehicular

295 exhaust and atmospheric photochemical reactions (Rogge et al., 1994; Rogge et al., 1993b; Schauer et
296 al., 1996; Zhang et al., 2002; Zhang et al. 2002; Fan et al. 2018). N-containing compounds were
297 identified in the samples, including heterocyclic compounds (alkyl-pyridines, alkyl-quinolines) and other
298 N-containing compounds (nitro, amine compounds). The average Σ alkyl-pyridines, Σ alkyl-quinolines
299 and Σ other N-containing compounds were 17.4 ± 7.58 , 16.6 ± 15.0 and 30.0 ± 23.1 ng m⁻³, respectively,
300 and the average total concentrations of N-containing compounds was 64.0 ng m⁻³, accounting for
301 approximately 0.2% of the OM.

302

303 The quinolines have been proposed for use as tracers of vehicular exhaust (Rogge et al., 1993a) and crude
304 oils and shale oil combustions (Schmitter et al., 1983; Simoneit et al., 1971), while the straight chain
305 alkyl-pyridines (n-Cn-pyridine) are related to petrochemical industries (Botalova et al., 2009) and
306 secondary formation from pyrolysis of proteins and amino acids under a high temperature (Chiavari and
307 Galletti, 1992; Hendricker and Voorhees, 1998; Kögel-Knabner, 1997). This study found that both
308 quinolines and alkyl-pyridines showed similar concentrations on the non-haze and haze days, 16.8 ± 16.5
309 ng m⁻³ (non-haze) and 16.5 ± 14.4 ng m⁻³ (haze days) and 12.0 ± 6.02 ng m⁻³ (non-haze days) and $15.3 \pm$
310 8.36 ng m⁻³ (haze days) respectively. Amino compounds can originate from biomass burning and coal
311 combustion, and are abundant in winter fine particulate matter samples compared to summer (Zhang et
312 al., 2002; Akyiiz 2008). In the present study, the average Σ other N-containing compounds was $34.2 \pm$
313 24.6 ng m⁻³ on the haze days, somewhat higher than 22.6 ± 19.4 ng m⁻³ on non-haze days.

314

315 The similar concentrations on the non-haze and haze days suggests that N-containing organic compounds
316 mainly originated from primary sources and subject to degradation during the haze formation process.

317

318 Tracers of tobacco smoke, benzoquinoline and isoquinoline have previously been determined in the PM

319 collected in Beijing, with concentrations of 3.10 and 0.22 ng m⁻³ respectively (Zhou et al., 2009). These
320 two compounds were also identified in the present study, with 4.40 and 0.80 ng m⁻³, respectively.
321 Phthalimide was identified in the PM at 0.91 ng m⁻³, and was considered to be derived from cyclization
322 and aromatization reactions of proteins or from intermediates in the transformation of carboxyl
323 ammonium salts to nitriles by Zhao et al. (2009).

324

325 **3.3.3 Esters**

326 Phthalate esters are organic chemicals that are commonly used in a variety of consumer products and in
327 various industrial and medical applications, and are predominantly used as plasticizers to improve the
328 flexibility of polyvinyl chloride (PVC) resins and other polymers. Table 1 shows a comparison of
329 phthalate esters (DBP, DEP, DEHP) between the present and previous studies in the winter in Beijing; it
330 seems that the concentrations of some phthalate esters have significantly decreased from earlier studies
331 (Wang et al., 2006; Zhou et al., 2009). The present study found that diisodecyl phthalates, DBP and
332 DEHP were abundant compounds in the ester group with 49.7 ± 43.2 , 16.9 ± 15.5 and 16.0 ± 12.6 ng m⁻³,
333 respectively. The DBP, DEP and DEHP in Beijing were far lower than that in winter in Tianjin (Kong
334 et al., 2013) and another fifteen cities around China (Li and Wang, 2015; Wang and Kawamura, 2005;
335 Wang et al., 2006). In addition, the average \sum Ester was 117 ± 82.1 ng m⁻³, with 132 ± 87.1 and $89.4 \pm$
336 70.0 ng m⁻³ on haze and non-haze days, respectively. Since phthalates are not chemically bound to the
337 polymeric matrix, they can enter the environment by escaping from manufacturing processes and by
338 leaching or vaporising from final products (Staples et al., 1997).

339

340 **3.3.4 PAHs, O-PAHs and alkylated-(PAHs & OPAHs)**

341 In all, 23 PAHs (2-6 rings), 19 oxygenated PAHs (O-PAHs) and 14 alkylated-(PAHs & OPAHs) were
342 determined in the PM_{2.5} samples. The average total polycyclic aromatic compounds (the sum of \sum PAHs,

343 Σ O-PAHs, Σ alkylated-(PAHs & OPAHs), alkyl-PHE and ANT and alkyl-NAP) was 569 ng m⁻³,
344 accounting for 1.88 % of OM.

345

346 The distribution of PAHs is shown in Figure 3; the most abundant PAHs were BbF, followed by CHR,
347 FLT, BaA and PYR. In all samples, the Σ PAHs ranged from 46.7-727 ng m⁻³ with average 281 \pm 176
348 ng m⁻³, accounting for 0.93 % of OM. In addition, the average Σ PAHs was 364 ng m⁻³ during haze days,
349 but only 159 ng m⁻³ on the non-haze days. It should be noted that retene was detected in most samples,
350 with an average concentration of 14.4 \pm 17.5 ng m⁻³. It has been suggested that retene predominantly
351 originates from the combustion of conifer wood (Simoneit et al., 1991).

352

353 Nineteen oxygenated PAHs (O-PAHs) make up of a class of PAH derivatives that are present in the
354 atmosphere as a result of direct emission during combustion and secondary formation by homogeneous
355 and heterogeneous photo-oxidation processes (Keyte et al., 2013; Ringuet et al., 2012). They are also of
356 scientific interest because they are, typically, found in the secondary organic aerosol (SOA) formed by
357 photo-oxidation of PAH (Shakya and Griffin, 2010). In urban samples, polycyclic aromatic ketones
358 (PAK), polycyclic aromatic quinones (PAQ) and polycyclic aromatic furanones (PAF) are typical groups
359 of compounds (Lin et al., 2015). The average total concentrations of O-PAH measured in this study
360 (Figure 4) was 67.9 ng m⁻³. The polycyclic aromatic ketones 4,5-pyrenequinone (4,5-PyrQ) (8.75 ng m⁻³)
361 and 1,6-pyrenequinone (1,6-PyrQ) (7.38 ng m⁻³) were the most abundant compounds during the
362 sampling campaign. Four O-PAHs have been identified previously at the PKU site in the 2012 heating
363 season in Beijing (Table 1); it is notable that the concentration of AQ was up to 108 ng m⁻³,
364 approximately 20 times that in the present study (5.12 ng m⁻³). As O-PAHs can be formed during
365 sampling, it is necessary to be very careful in reconciling their presence with specific sources (Pitts et al.,
366 1980). The average Σ O-PAHs was 86.5 ng m⁻³ during haze days, but 39.7 ng m⁻³ on the non-haze days.

367 The ratio of quinone: parent PAH has been used to assess the air mass age (Alam et al., 2014; Harrison
368 et al., 2016). The average ratios of phenanthraquinone to phenanthrene (PQ:PHE), anthraquinone to
369 anthracene (AQ:ANT) and benzo(a)anthracene-7,12-quinone to benzo(a)anthracene (BaAQ:BaA) were
370 0.37, 1.27, 0.32, respectively, with PQ:PHE, AQ:ANT and BaAQ:BaA ratios of 0.25, 0.88 and 0.26 on
371 the haze days, which were lower than 0.55, 1.92, 0.40 on non-haze days. The BaAQ:BaA ratios were
372 lower than earlier published data of 1.28 measured in Beijing (Li et al., 2019), 1.40 in Xian (Wang et al.,
373 2016) and 0.54 in Beijing-Tianjing (Wang, 2010), but higher than the 0.08 measured in Guangzhou (Wei
374 et al., 2012) and 0.09 in Zhuanghu (Ding et al., 2012). Shen et al. (2011) reported that the BaAQ:BaA
375 ratio was 0.03 for coal combustion, 0.16 for crop residue burning (Shen et al., 2012a) and 6.6 from
376 biomass pellet burning (Shen et al., 2012b). The low ratios of O-PAHs/PAHs in our data probably
377 indicated that the particulate matter mainly originated from coal combustion and biomass burning.
378 However, the lower ratios on haze days than non-haze days may imply continued oxidation of the O-
379 PAH to products which were not analysed. Li et al. (2019) also reported that ratios of Σ OPAH to Σ PAH
380 were very similar during haze and clean air periods, which provides support for this conclusion.

381

382 **3.3.5 Molecular markers**

383 The hopanes are compounds present in crude oil as a result of the decomposition of sterols and other
384 biomass and are not by-products of combustion (Simoneit, 1985). They are very stable and have been
385 proposed for use as tracers for atmospheric particles from fossil fuel combustion, such as motor vehicle
386 exhaust (Simoneit, 1985) and coal combustion (Oros and Simoneit, 2000). The hopanes are widely used
387 as tracers of traffic emission due to vehicle emissions having high loadings of hopanes (Cass, 1998). The
388 comparison of hopanes between this study and previous studies in the winter or heating season of Beijing
389 are shown in Table 1. Hopanes were extensively present in Beijing PM_{2.5} samples, and their carbon
390 numbers ranged from C₂₇ to C₃₂, but not C₂₈ (Table 2). The average concentration of hopanes in Beijing

391 was $32.7 \pm 24.7 \text{ ng m}^{-3}$, with $15.2 \pm 10.7 \text{ ng m}^{-3}$ and $44.6 \pm 24.6 \text{ ng m}^{-3}$ on non-haze and haze days,
392 respectively. Previous studies have found that C₂₉ (17a(H), 21h(H)-norhopane) was dominant in the
393 hopane series and consistent with that from coal combustion (He et al., 2006a), while C₃₀ (17β(H)21α(H)-
394 hopane and 17a(H), 21β(H)-hopane) was similar to C₂₉ in the winter time in Beijing and attributed to
395 gasoline and diesel exhaust (Simoneit, 1985).

396

397 Levoglucosan and methoxyphenols from pyrolysis of cellulose and lignin are usually used as unique
398 tracers for biomass burning in source apportionment models (Schauer and Cass, 2000). Levoglucosan
399 (1,6-anhydro-β-D-glucopyranose) has been for a long time employed as the specific molecular marker
400 for long-range transport of biomass burning aerosol, based on its high emission factors and assumed
401 chemical stability (Fraser and Lakshmanan, 2000; Simoneit et al., 2000). It is a highly abundant
402 compound and the concentrations in winter in Beijing have a significant fluctuation (Table 1). The
403 average \sum levoglucosan was $355 \pm 232 \text{ ng m}^{-3}$ during the entire sampling period, and $417 \pm 223 \text{ ng m}^{-3}$
404 in haze episodes, approximately twofold that of the non-haze days, $238 \pm 193 \text{ ng m}^{-3}$, indicating a
405 significant impact of biomass burning upon wintertime aerosols in Beijing.

406

407 Methoxyphenols are usually also considered as tracers for wood burning (Simpson et al., 2005; Yee et
408 al., 2013) with the average \sum Methoxyphenols $7.29 \pm 7.11 \text{ ng m}^{-3}$, and the haze days ($9.03 \pm 7.93 \text{ ng m}^{-3}$)
409 twofold greater than non-haze days ($4.74 \pm 4.95 \text{ ng m}^{-3}$) during the campaigns. In Beijing and its
410 surrounding areas, harvest occurs in late September to October for corn, and biomass fuels are used for
411 cooking and heating purpose in the winter. However, the methoxyphenols are abundant components in
412 the smoke from broad-leaf tree and shrub burning (Wang et al., 2009), and have been identified in all
413 coal smoke (Simoneit, 2002a), so cannot be used as source-specific markers for biomass burning.

414

415 Phenolic compounds from the thermal degradation of lignin have been proposed as potentially useful
416 tracers for wood smoke, and many of them are emitted in relatively high quantities and are specific to
417 wood combustion sources (Simoneit, 2002b; Simoneit et al., 2004). Another important source of phenolic
418 compounds is oxidation of monoaromatic compounds and PAHs (Pan and Wang, 2014). Phenols and
419 naphthalenol were identified in the PM_{2.5}, with the average \sum phenolic compounds $21.6 \pm 17.0 \text{ ng m}^{-3}$,
420 with $14.0 \pm 13.2 \text{ ng m}^{-3}$ and $25.9 \pm 17.9 \text{ ng m}^{-3}$ on the non-haze and haze days, respectively. However, it
421 is notable that the concentrations of naphthalenol identified in the present study were far lower than that
422 of previous studies (Table 1).

423

424 Pristane (Pr) and phytane (Ph) have been found in the exhaust of petrol and diesel engines and in
425 lubricating oil, indicating their origin from petroleum (Simoneit, 1984). Since their presence is ubiquitous
426 in vehicle exhausts and negligible in contemporary biogenic sources in urban environments, they can be
427 used as petroleum tracers for airborne particulate matter. The mean values of Pr and Ph in our samples
428 are 2.24 and 1.94 ng m^{-3} , respectively. Biogenic inputs are often characterised by a predominance of the
429 odd carbon alkanes and Pr. Since Ph is rarely found in biological material, most biological hydrocarbons
430 have a Pr/Ph ratio far higher than 1.0 (Oliveira et al., 2007), but values approaching unity indicate a
431 hydrocarbon signature derived from petrochemical use. The average Pr/Ph ratios were 1.15 for PM_{2.5}
432 samples, and this finding is quite similar to the results from the southern Chinese city of Guangzhou, 1.1-
433 1.8 (Bi et al., 2002), but almost four times greater than Beijing summer samples (0.3) (Simoneit et al.,
434 1991). The high Pr/Ph indicated that the hydrocarbons in urban aerosol derive mainly from petroleum
435 residues probably deriving from vehicular emissions in Beijing.

436

437 **3.4 The Molecular Distributions of Aliphatic Hydrocarbons**

438 Figure 4 shows the molecular distributions of aliphatic hydrocarbons on non-haze and haze days. The

439 details on the n-alkanes are given by Lyu et al. (2019). Briefly, the Σ n-alkanes (C_{10} - C_{36}) ranged from
440 42.4 to 1241 ng m^{-3} with an average $450 \pm 316 \text{ ng m}^{-3}$, and the average Σ n-alkanes was 577 ng m^{-3} during
441 haze episodes, more than twice that of the non-haze period (264 ng m^{-3}). The n-alkanes (C_{20} - C_{31}) were
442 the most abundant homologues (Figure 4), accounting for approximately 83% of the Σ n-alkanes.

443

444 The total concentrations of branched alkanes (C_{12} - C_{36}) ranged from 125-647 ng m^{-3} with the average 356
445 $\pm 173 \text{ ng m}^{-3}$ during the sampling period. The average branched alkanes concentration was $440 \pm 144 \text{ ng}$
446 m^{-3} during all haze episodes, which was higher than $234 \pm 138 \text{ ng m}^{-3}$ on the non-haze days. The most
447 abundant branched alkanes were observed at C_{22} , with the average concentration of 29.2 ng m^{-3} , and the
448 greatest abundance of branched alkanes groups was observed within the carbon atom range of C_{20} - C_{30} ,
449 accounting for 67.7% of Σ branched alkanes. The branched alkanes have lower concentrations than n-
450 alkanes when the carbon number is $>C_{20}$ on haze and non-haze days, while showing higher
451 concentrations than n-alkanes when the carbon number is lower than C_{19} .

452

453 It is difficult to identify the potential sources of branched alkanes from the literature, although Alam et
454 al. (2016b) reported that branched alkanes (C_{11} - C_{33}) were an abundant compound group in diesel exhaust.
455 The increase of high molecular weight branched alkanes (C_{20} - C_{30}) from non-haze days to haze days is
456 consistent with a primary emission source, probably linked to coal combustion or vehicular emissions.
457 The fact that both n-alkanes and branched alkanes increase quite similarly between non-haze and haze
458 conditions is consistent with them arising from the same source(s), or sources with highly correlated
459 emissions.

460

461 Other groups of aliphatic and alicyclic compounds identified in the $\text{PM}_{2.5}$, include alkyl-decalins, alkyl-
462 pyridines, alkyl-furanones, alkyl-cyclohexanes and alkyl-benzenes. Figure 5 shows the molecular

463 distributions of these series of compounds. Engine studies (Alam et al., 2016b) have also found that
464 compounds observed in vehicle exhaust beside n-alkanes and PAHs, include straight and branched
465 cyclohexanes (C₁₁-C₂₅), various cyclic aromatics, alkyl-decalins and alkyl-benzenes. The particle-bound
466 n-C_n-cyclohexanes with carbon numbers from C₁₂ to C₂₆ were identified in diesel exhaust (Alam et al.,
467 2016b) with a dominant range C₁₈-C₂₅, and the total (particle + gas) concentration of n-C_n-cyclohexanes
468 was 2.05 μg m⁻³. The n-C_n-cyclohexanes (C₂₀-C₃₀) were identified at the IAP site with average Σ n-C_n-
469 cyclohexane 39.4 ± 37.1 ng m⁻³. The most abundant range was observed at C₂₂-C₂₇, highly consistent
470 with the engine study, implying a significant contribution from vehicle emissions. In addition, the
471 average Σ n-C_n-cyclohexane (C₂₀-C₃₀) was 53.3 ± 39.3 ng m⁻³ during haze episodes, approximately five
472 times higher than 10.8 ± 8.22 ng m⁻³ in the non-haze period, a larger ratio than for other primary emissions.
473 The alkyl-decalins and tetralin are products obtained by hydrogenation of naphthalene and its derivatives
474 during the refining process and have been identified in vehicle exhaust (Afzal et al., 2008; Alam et al.,
475 2016b; Ogawa et al., 2007). The average Σ alkyl-decalins was 110 ng m⁻³, with 85.4 ± 65.5 and 126 ±
476 110 ng m⁻³ on non-haze and haze days respectively. The Σ n-C_n-benzene (C₁₆-C₂₅) identified in the
477 samples ranged from 7.71 to 410 ng m⁻³ with an average of 56.6 ± 73.0 ng m⁻³. The average Σ n-C_n-
478 benzene (C₁₆-C₂₅) was 77.2 ± 88.2 ng m⁻³ during haze episodes, approximately four times the 23.3 ± 15.1
479 ng m⁻³ of the non-haze period. Other alkyl-benzenes (C₉-C₂₅) were also identified and have higher
480 concentrations at C₁₂, especially for the non-haze days.

481

482 **3.5 Distribution of Compounds with respect to Volatility and Polarity, and the Estimation of** 483 **Unidentified Mass**

484 The method for characterising the volatility/polarity distribution of compounds is detailed in the
485 Supporting Information. Briefly, the chromatography image was separated into seven parts according to
486 the main chemical and physical properties of the organic compounds and the distribution of internal

487 standards (IS), and the detailed protocol is shown in Table S4. The diagram of the separated image with
488 seven parts is shown in Figure 6a, and the concentrations measured in each part are shown in Figure 6
489 and Table 3. In the chromatogram (Figure 6), volatility decreases from left to right and polarity increases
490 from bottom to top. Table 3 shows the estimated mass concentration of all components of the
491 chromatogram, alongside the amount of mass not accounted for by the specific compounds reported in
492 this paper.

493

494 For the non-haze days, the sum of identified organic compounds (IOC) with carbon numbers higher than
495 C₆ was 1.84 μg m⁻³, accounting for 46.5 % of total organic compounds. The IOC of the haze days was
496 almost two times that of non-haze periods, with an average of 3.42 μg m⁻³, accounting for 46.3% of total
497 measured organic matter. In addition, the sum of unidentified compounds increased from 2.12 μg m⁻³ on
498 non-haze days to 3.96 μg m⁻³ on haze days, accounting for 53.5 % and 53.7% of total measured organic
499 matter, respectively. Hence there is no marked difference in the proportions of identified and unidentified
500 compounds between haze and non-haze conditions.

501

502 For the non-haze days, Section 1 of the chromatogram has the highest concentration of 802 ng m⁻³,
503 followed by Section 7 (792 ng m⁻³), accounting for 20.3 % and 20.0 % of the total organic compounds
504 respectively, implying that both low molecular weight (LMW) hydrocarbons (Section 1) and high
505 molecular weight (HMW) PAHs (Section 7, 3~6 rings) and compounds of similar volatility/polarity were
506 the main organic components of atmospheric particulate matter measurable by the GCxGC separation
507 technique. The PAHs are important organic compounds appearing in Sections 6 + 7, accounting for 32.3%
508 of total measured organic compounds during the non-haze days. Sections 2, 3 and 4 showed relatively
509 low concentrations, and medium molecular weight hydrocarbons in the range of C₂₃~C₂₇ (Section 3) were
510 the more abundant aliphatic hydrocarbons relative to Section 2 (C₁₇~C₂₃) and Section 4 (>C₂₇), probably

511 caused by primary emissions from vehicular and coal combustion (Cao et al., 2018). Section 5 contains
512 oxidized monoaromatic compounds, and the concentrations were higher than Section 6 (mainly
513 containing naphthalene derivatives) and lower than Section 1, probably mainly arising from vehicular
514 emissions or oxidized from the monoaromatic precursors (Section 1) (Schwantes et al., 2017).

515

516 The polarity distribution characteristics of atmospheric organic compounds on the non-haze days were
517 also studied. For the volatile areas, low polarity compounds (Section 1) have a lower concentration than
518 polar compounds (Sections 5 + 6) during the non-haze days. On the contrary, for the semi-and non-
519 volatile area, the sum of low polar compounds (Sections 2 + 3 + 4) have higher concentrations than polar
520 organic compounds (Section 7).

521

522 The concentrations in all sections increased from non-haze to haze days, and the main difference between
523 haze and non-haze days attaches to Sections 5, 6 and 7 (Figure 6b), indicating a more polar aerosol during
524 periods of haze. Section 6 has the highest concentrations on the haze days (1556 ng m^{-3}), increased more
525 than three times on the haze days in contrast to non-haze days (485 ng m^{-3}), followed by Section 7 (1337
526 ng m^{-3}) and Section 5 (1309 ng m^{-3}), indicating that the oxidized monoaromatics, naphthalene derivatives
527 and oxidized HMW PAHs were the main identified components of the atmospheric particulate matter
528 during the haze days. The concentrations were compared among the seven sections, and the highest
529 concentrations of Section 6 were probably contributed by the degradation of HMW PAHs (from Section
530 7). For the oxidized monoaromatic compounds (Section 5), the degradation of naphthalene derivatives
531 was probably a major contributor, but not compounds oxidized from Section 1. The concentrations of
532 Section 3 were also observed to increase from non-haze days (573 ng m^{-3}) to haze days (1060 ng m^{-3}),
533 indicating that accumulation has an obvious effect on the stable compounds with carbon number between
534 C_{23} to C_{27} during haze formation under low wind speed (Table S1).

535 3.6 Elevation of Primary and Secondary Constituents during Haze Events

536 By definition, concentrations of PM_{2.5} are elevated during haze events, but the question arises as to
537 whether primary or secondary organic compounds make a larger contribution to the rise in concentrations.
538 Constituents that are expected to be primary are typically elevated in mean concentration by a factor of
539 around two (Table S3). Examples are n-alkanes (ratio of haze : non-haze of 2.2), levoglucosan (1.8) and
540 hopanes (2.9). This is consistent with the ratios for primary gaseous emissions, including SO₂ (ratio of
541 2.6), CO (2.5) and NO_x (2.2) (Table S1). Surprisingly, however, both BC (ratio of 3.8) and EC (3.4)
542 (Table S1) are primary constituents with a large haze:non-haze ratio, comparable to that of PM_{2.5} mass
543 (4.0). Consequently the factors leading to an elevation of concentrations during the haze appear complex
544 and are likely to be resolved fully only by chemistry-transport models.

545

546 OC/EC ratios are used to estimate the relative contribution of primary and secondary sources; high
547 OC/EC ratios (> 2.0) have been observed for aerosols with significant SOA contributions in Beijing (Lv
548 et al., 2019; Ji et al., 2018). The OC/EC ratio in this study was 3.88 on average, suggesting a significant
549 contribution of SOA in Beijing aerosols, which is consistent with the results of Section 3.5. The aliphatic
550 carbonyls, which have both primary and secondary sources (Lyu et al., 2018a,b) range from ratios of 1.6
551 (n-alkanals) to 2.8 (n-alkan-2-ones). This result was consistent with Section 3.5; it was found that the
552 chromatogram Sections 2 and 3 which contained alkanals (C₁₅≤C_n≤C₂₅) and alkanones (C₁₅≤C_n≤C₂₅)
553 have slightly higher concentrations on haze days than non-haze days. However, the low ratio alkanal and
554 alkanone compounds are quite readily oxidised (Chacon-Madrid et al., 2010; Chacon-Madrid and
555 Donahue, 2011), and a low ratio may reflect a high degree of further processing to form more oxidised
556 species on the haze days compensating for enhanced formation.

557

558 There are no compounds in Table S3 certain to be exclusively secondary. However, the results in Figure

559 6 show an appreciable elevation in more polar compounds (upper part of the chromatogram) on haze
560 days, suggestive of a greater relative abundance of more oxidised, possibly secondary compounds in the
561 haze. The ratio of average PM_{2.5} mass between haze and non-haze days was 4.0, and organic carbon, 2.7
562 (Table S1). The ratio for organic matter would be greater than 2.7, due to a higher OM/OC ratio in
563 secondary compounds. This is strongly suggestive of a greater contribution from an elevation in
564 secondary than primary species concentrations during the haze events, and that much of the mass lies
565 outside of the chromatogram due to the low volatility of the secondary species.

566
567
568

4. CONCLUSIONS

569 Over 300 polar and non-polar organic compounds were determined in the fine particle samples from
570 Beijing, and these compounds have been grouped into more than twenty classes, including normal and
571 branched alkanes, n-alkenes, aliphatic carbonyl compounds (1-alkanals, n-alkan-2-ones and n-alkan-3-
572 ones), n-alkanoic acids, n-alkanols, PAHs, oxygenated PAHs (O-PAHs), alkylated-(PAHs & OPAHs),
573 hopanes, n-C_n-benzene, alkyls-benzenes, n-C_n-cyclohexane, pyridines, quinolines, furanones, and
574 biomarkers (levoglucosan, cedrol, phytane, pristane, supraene and phytone). The total concentrations of
575 identified organic compounds ranged from 0.94 to 5.14 $\mu\text{g m}^{-3}$ with an average of $2.84 \pm 1.19 \mu\text{g m}^{-3}$,
576 accounting for 9.40 % of OM mass. The six groups which accounted for 66% of total identified organic
577 compound mass included n-alkanes, levoglucosan, branched-alkanes, PAHs, n-alkenes and alkyl-
578 benzenes, and these were significantly impacted by primary emission sources. In addition, the average
579 total polycyclic aromatic compounds (the sum of \sum PAHs, \sum O-PAHs, \sum alkylated-(PAHs & OPAHs),
580 alkyl-PHE and ANT and alkyl-NAP) was 560 ng m^{-3} , accounting for 1.88 % of OM. The comparisons
581 of identified groups between non-haze and haze periods showed that most organic compound groups
582 have a higher concentration on the haze days relative to the non-haze days. The average sum of the
583 identified compounds increased from 1.84 $\mu\text{g m}^{-3}$ to 3.42 $\mu\text{g m}^{-3}$ from non-haze days to haze days. A

584 unimodal molecular distribution of alkanes was observed in the range from C₈ to C₃₆, and these
585 compounds make significant contributions to atmospheric organic compounds in the range of C₁₉-C₂₈,
586 especially on the haze days. The unidentified compounds in the chromatogram were estimated, and the
587 results show that the average sum of unidentified compounds increased from 2.12 μg m⁻³ on non-haze
588 days to 3.96 μg m⁻³ on haze days, accounting approximately for 53.5 % and 53.7% of total organic
589 compounds, respectively. Finally, the total mass concentrations of measured organic compounds (≥C₆)
590 was 3.96 μg m⁻³ and 7.39 μg m⁻³ on the non-haze and haze days, accounting for 26.4% and 18.5% of OM
591 mass, respectively on these days. The remaining mass is that which is not volatile under the conditions
592 of the gas chromatography. The higher percentage of non-GC-volatile organic matter on haze days is
593 indicative of a greater degree of oxidation of the organic aerosol, consistent with the difference in the
594 chromatogram between haze and non-haze days. The greater contribution of secondary constituents
595 during haze events has been reported previously by Huang et al. (2014) and Ma et al. (2017), but not the
596 greater extent of oxidation of organic matter. In a modelling study, Li et al. (2017) found that during
597 winter haze conditions in Beijing the majority of secondary PM_{2.5} had formed one or more days prior to
598 arrival, hence explaining its highly oxidised condition.

599

600 **DATA ACCESSIBILITY**

601 Data supporting this publication are openly available from the UBIRA eData repository at
602 <https://doi.org/10.25500/edata.bham.00000303>.

603

604 **AUTHOR CONTRIBUTIONS**

605 The study was conceived by RMH and ZS and the fieldwork was organised and supervised by ZS and
606 PF. TV and DL undertook air sampling work and general data analyses for the campaign while RL
607 carried analytical work on the Beijing samples under the guidance of MSA and CS. XW contributed

608 analyses of data from London. RL produced the first draft of the manuscript with guidance from YF and
609 RMH and all authors contributed to the refinement of the submitted manuscript.

610

611 **ACKNOWLEDGEMENTS**

612 Primary collection of samples took place during the APHH project in which our work was funded by the
613 Natural Environment Research Council (NERC) (NE/N007190/1). The authors would also like to thank
614 the China Scholarship Council (CSC) for support to R.L.

615

616 **COMPETING INTERESTS**

617 The authors have no conflict of interest.

618

619 **REFERENCES**

620

621 Afzal, A., Chelme-Ayala, P., El-Din, A. G., El-Din, M. G.: Automotive Wastes, *Water Environ., Res.*,
622 80, 1397-1415, 2008.

623

624 Akyüz, M.: Simultaneous determination of aliphatic and aromatic amines in ambient air and airborne
625 particulate matters by gas chromatography-mass spectrometry, *Atmos. Environ.*, 42, 3809-3819, 2008.

626

627 Alam, M. S., Zeraati-Rezaei, S., Liang, Z., Stark, C., Xu, H., MacKenzie, A. R., Harrison, R. M.:
628 Mapping and quantifying isomer sets of hydrocarbons ($\geq C_{12}$) in diesel exhaust, lubricating oil and
629 diesel fuel samples using GC \times GC-ToF-MS, *Atmos. Meas. Tech.*, 11, 3047, 2018.

630

631 Alam, M. S., Stark, C., Harrison, R. M.: Using variable ionisation energy time-of-flight mass
632 spectrometry with comprehensive GC \times GC to identify isomeric species, *Anal. Chem.*, 88, 4211-4220,
633 2016a.

634

635 Alam, M. S., Zeraati-Rezaei, S., Stark, C. P., Liang, Z., Xu, H., Harrison, R. M.: The characterisation
636 of diesel exhaust particles - composition, size distribution and partitioning, *Faraday. Discuss.*, 189, 69-
637 84, 2016b.

638

639 Alam, M. S., Harrison R. M.: Recent advances in the application of 2-dimensional gas chromatography
640 with soft and hard ionisation time-of-flight mass spectrometry in environmental analysis, *Chem. Sci.*, 7,
641 3968-3977, 2016.

642

643 Alam, M., Delgado-Saborit, J. M., Stark, C., Harrison, R. M.: Investigating PAH relative reactivity
644 using congener profiles, quinone measurements and back trajectories, *Atmos. Chem. Phys.*, 14, 2467-
645 2477, 2014.

646

647 Bi, X., Sheng, G., Peng, P.A., Zhang, Z., Fu, J.: Extractable organic matter in PM₁₀ from LiWan
648 District of Guangzhou City, PR China, *Sci. Tot. Environ.*, 300, 213-228, 2002.

649

650 Botalova, O., Schwarzbauer, J., Frauenrath, T., and Dsikowitzky, L.: Identification and chemical
651 characterization of specific organic constituents of petrochemical effluents, *Water Res.*, 43, 3797-3812,
652 2009.

653

654 Cao, R., Zhang, H., Geng, N., Fu, Q., Teng, M., Zou, L., Gao, Y., and Chen, J.: Diurnal variations of
655 atmospheric polycyclic aromatic hydrocarbons (PAHs) during three sequent winter haze episodes in
656 Beijing, China, *Sci. Tot. Environ.*, 625, 1486-1493, 2018.

657

658 Cass, G. R.: Organic molecular tracers for particulate air pollution sources. *TrAC Trends Anal. Chem.*,
659 17, 356-366, 1998.

660

661 Chacon-Madrid, H. J., and Donahue, N.: Fragmentation vs. functionalization: chemical aging and
662 organic aerosol formation, *Atoms. Chem. Phys.*, 11, 10553-10563, 2011.

663

664 Chacon-Madrid, H. J., Presto, A. A., and Donahue, N. M.: Functionalization vs. fragmentation: n-
665 aldehyde oxidation mechanisms and secondary organic aerosol formation, *Phys. Chem. Chem. Phys.*,
666 12, 13975-13982, 2010.

667
668 Chiavari, G., Galletti, G. C.: Pyrolysis - gas chromatography/mass spectrometry of amino acids,
669 J.Anal.Appl. Pyrol., 24, 123-137, 1992.
670
671 Ding, J., Zhong, J., Yang, Y., Li, B., Shen, G., Su, Y., Chen, W., Shen, H., Wang, B., and Rong, W.:
672 Occurrence and exposure to polycyclic aromatic hydrocarbons and their derivatives in a rural chinese
673 home through biomass fuelled cooking, Environ. Pollut., 169, 160-166, 2012.
674
675 Fan, X., Wei, S., Zhu, M., Song, J., Peng, P. A.: Molecular characterization of primary humic-like
676 substances in fine smoke particles by thermochemolysis–gas chromatography–mass spectrometry,
677 Atmos. Environ., 180, 1-10, 2018.
678
679 Fraser, M. P., Lakshmanan, K.: Using levoglucosan as a molecular marker for the long-range transport
680 of biomass combustion aerosols, Environ. Sci. Technol., 34, 4560-4564, 2000.
681
682 Gao, Y., Guo, X., Ji, H., Li, C., Ding, H., Briki, M., Tang, L., Zhang, Y.: Potential threat of heavy
683 metals and PAHs in PM_{2.5} in different urban functional areas of Beijing, Atmos. Res., 178, 6-16,
684 2016.
685
686 Guo, S., Hu, M., Guo, Q., Zhang, X., Schauer, J., Zhang, R.: Quantitative evaluation of emission
687 controls on primary and secondary organic aerosol sources during Beijing 2008 Olympics, Atmos.
688 Chem. Phys., 13, 8303-8314, 2013.
689
690 Hamilton, J., Webb, P., Lewis, A., Hopkins, J., Smith, S., Davy, P.: Partially oxidised organic
691 components in urban aerosol using GCXGC-TOF/MS. Atmos. Chem. Phys., 4, 1279-1290, 2004.
692
693 Haque, M., Kawamura, K., Deshmukh, D. K., Fang, C., Song, W., Mengying, B., and Zhang, Y.-L.:
694 Characterization of organic aerosols from a Chinese megacity during winter: predominance of fossil
695 fuel combustion, Atmos. Chem. Phys., 19, 5147-5164, 2019.
696
697 Harrison, R. M., Alam, M.S., Dang, J., Ismail, I., Basahi, J., Alghamdi, M. A., Hassan, I., Khoder, M.:
698 Relationship of polycyclic aromatic hydrocarbons with oxy (quinone) and nitro derivatives during air
699 mass transport, Sci. Tot. Environ., 572, 1175-1183, 2016.
700
701 He, L.-Y., Hu, M., Huang, X.-F., Zhang, Y.-H., Tang, X.-Y.: Seasonal pollution characteristics of
702 organic compounds in atmospheric fine particles in Beijing, Sci. Tot. Environ., 359, 167-176, 2006a.
703
704 He, L.-Y., Hu, M., Huang, X.-F., Zhang, Y.-H., Tang, X.-Y.: Seasonal pollution characteristics of
705 organic compounds in atmospheric fine particles in Beijing, Sci. Tot. Environ., 359, 167-176, 2006b.
706
707 Hendricker, A. D., Voorhees, K. J.: Amino acid and oligopeptide analysis using Curie-point pyrolysis
708 mass spectrometry with in-situ thermal hydrolysis and methylation: mechanistic considerations, J.
709 Anal. Appl. Pyrol., 48, 17-33, 1998.
710
711 Huang, R.-J., Zhang Y., Bozzetti, C., Ho, F.-H., Cao, J.-J., Han, Y., Daellenbach, K. R., Slowik, J. G.,
712 Platt, S. M., Canonaco, F., Zotter, P., Wolf, R., Pieber, S. M., Brun, E. A., Crippa, M., Ciarelli, G.,
713 Piazzalunga, A., Schwikowski, M., Abbaszade, G., Schnelle-Kreis, J., Zimmermann, R., An, Z., Szidat,

714 S., Baltensperger, U., El Haddad, I., Prevot, A. S. H.: High secondary aerosol contribution to
715 particulate pollution during haze events in China, *Nature* 514, 218-222, 2014.

716 Huang, X.-F., He, L.-Y., Hu, M., Zhang, Y.-H.: Annual variation of particulate organic compounds in
717 PM_{2.5} in the urban atmosphere of Beijing, *Atmos. Environ.*, 40, 2449-2458, 2006.

718

719 Keyte, I. J., Harrison, R. M., Lammel, G.: Chemical reactivity and long-range transport potential of
720 polycyclic aromatic hydrocarbons—a review, *Chem. Soc.Rev.*, 42, 9333-9391, 2013.

721

722 Ji, D., Yan, Y., Wang, Z., He, J., Liu, B., Sun, Y., Gao, M., Li, Y., Cao, W., Cui, Y., Hu, B., Xin, J.,
723 Wang, L., Liu, Z., Tang, G., and Wang, Y.: Two-year continuous measurements of carbonaceous
724 aerosols in urban Beijing, China: Temporal variations, characteristics and source analyses, *Chemosphere*
725 200, 191-200, 2018.

726

727 Kögel-Knabner, I.: ¹³C and ¹⁵N NMR spectroscopy as a tool in soil organic matter studies, *Geoderma*
728 80, 243-270, 1997.

729

730 Kong, S., Ji, Y., Liu, L., Chen, L., Zhao, X., Wang, J., Bai, Z., Sun, Z.: Spatial and temporal variation
731 of phthalic acid esters (PAEs) in atmospheric PM₁₀ and PM_{2.5} and the influence of ambient temperature
732 in Tianjin, China, *Atmos. Environ.*, 74, 199-208, 2013.

733

734 Lang, J., Zhang, Y., Zhou, Y., Cheng, S., Chen, D., Guo, X., Chen, S., Li, X., Xing, X., Wang, H.:
735 Trends of PM_{2.5} and chemical composition in Beijing, 2000-2015, *Aerosol Air Qual. Res.*, 17, 412-425,
736 2017.

737

738 Li, L. J., Ho, S. S. H., Feng, B., Xu, H., Wang, T., Wu, R., Huang, W., Qu, L., Wang, Q., and Cao, J.:
739 Characterization of particulate-bound polycyclic aromatic compounds (PACs) and their oxidations in
740 heavy polluted atmosphere: A case study in urban Beijing, China during haze events, *Sci. Tot.*
741 *Environ.*, 660, 1392-1402, 2019.

742

743 Li, J., Du, H., Wang, Z., Sun, Y., Yang, W., Li, J., Tang, X., Fu, P.: Rapid formation of a severe
744 regional winter haze episode over a mega-city cluster on the North China Plain, *Environ. Pollut.*, 223,
745 605-615, 2017

746

747 Lin, Y., Ma, Y., Qiu, X., Li, R., Fang, Y., Wang, J., Zhu, Y., Hu, D.: Sources, transformation, and
748 health implications of PAHs and their nitrated, hydroxylated, and oxygenated derivatives in PM_{2.5} in
749 Beijing, *J. Geophys. Res. Atmos.*, 120, 7219-7228, doi:10.1002/2015JD023628, 2015.

750

751 Lv, D., Chen, Y., Zhu, T., Li, T., Shen, F., and Li X.: The pollution characteristics of PM₁₀ and PM_{2.5}
752 during summer and winter in Beijing, Suning and Islamabad, *Atmos. Pollut. Res.*, in press,
753 <https://doi.org/10.1016/j.apr.2019.01.021>, 2019.

754

755 Lyu, R., Shi, Z., Alam, M. S., Wu, X., Liu, D., Vu, T. V., Stark, C., Fu, P., Feng, Y., and Harrison, R.
756 M.: Alkanes and aliphatic carbonyl compounds in wintertime PM_{2.5} in Beijing, China, *Atmos. Environ.*,
757 202, 244-255, 2019.

758

759 Lyu, R., Alam, M. S., Stark, C., Xu, R., Shi, Z., Feng, Y., Harrison, R. M.: Aliphatic Carbonyl
760 Compounds (C₈-C₂₆) in Wintertime Atmospheric Aerosol in London, UK, *Atmos. Chem. Phys.*,
761 submitted, 2018a.

762 Lyu, R., Shi, Z., Alam, M. S., Wu, X., Liu, D., Vu, T. V., Stark, C., Fu, P., Feng, Y., Harrison R. M.:
763 Alkanes and aliphatic carbonyl compounds in wintertime PM_{2.5} in Beijing, China, *Atmos. Environ.*,
764 submitted, 2018b.
765

766 Ma, Y., Cheng, Y., Qiu, X., Cao, G., Fang, Y., Wang, J., Zhu, T., Yu, J., Hu, D.: Sources and oxidative
767 potential of water-soluble humic-like substances (HULIS WS) in fine particulate matter (PM_{2.5}) in
768 Beijing, *Atmos. Chem. Phys.*, 18, 5607-5617, 2018.
769

770 Ma, Q., Wu, Y., Zhang, D., Wang, X., Xia, Y., Liu, X., Tian, P., Han, Z., Xia, X., Wang, Y., Zhang,
771 R.: Roles of regional transport and heterogeneous reactions in the PM_{2.5} increase during winter haze
772 episodes in Beijing, *Sci. Tot. Environ.*, 599-600, 246-253, 2017.
773

774 Ogawa, H., Ibuki, T., Minematsu, T., Miyamoto, N.: Diesel combustion and emissions of decalin as a
775 high productivity gas-to-liquid fuel, *Energy & Fuels*, 21, 1517-1521, 2007.
776

777 Oliveira, T. S., Pio, C., Alves, C. A., Silvestre, A. J., Evtyugina, M., Afonso, J., Fialho, P., Legrand, M.,
778 Puxbaum, H., Gelencsér, A.: Seasonal variation of particulate lipophilic organic compounds at nonurban
779 sites in Europe. *J. Geophys. Res.: Atmospheres*, 112., D23S09, doi:10.1029/2007JD008504, 2007.
780

781 Oros, D., Simoneit, B.: Identification and emission rates of molecular tracers in coal smoke particulate
782 matter, *Fuel* 79, 515-536, 2000.
783

784 Pan, S., Wang, L.: Atmospheric oxidation mechanism of m-xylene initiated by OH radical, *J. Phys.*
785 *Chem. A*, 118, 10778-10787, 2014.
786

787 Pitts, J. N., Lokensgard, D. M., Ripley, P. S., Van Cauwenberghe, K. A., Van Vaeck, L., Shaffer, S. D.,
788 Thill, A. J., Belser, W. L.: Atmospheric epoxidation of benzo[a]pyrene by ozone: Formation of the
789 metabolite benzo[a]pyrene-4, 5-oxide, *Science*, 210, 1347-1349, 1980.
790

791 Ren, L., Fu, P., He, Y., Hou, J., Chen, J., Pavuluri, C.M., Sun, Y., Wang, Z.: Molecular distributions
792 and compound-specific stable carbon isotopic compositions of lipids in wintertime aerosols from
793 Beijing, *Scientific Rep.*, 6, 27481, 2016.
794

795 Ringuet, J., Albinet, A., Leoz-Garziandia, E., Budzinski, H., Villenave, E.: Reactivity of polycyclic
796 aromatic compounds (PAHs, NPAHs and OPAHs) adsorbed on natural aerosol particles exposed to
797 atmospheric oxidants, *Atmos. Environ.*, 61, 15-22, 2012.
798

799 Rogge, W. F., Hildemann, L. M., Mazurek, M. A., Cass, G. R., Simoneit, B. R.T .. Sources of Fine
800 Organic Aerosol. 6. Cigaret Smoke in the Urban Atmosphere, *Environ.Sci.Technol.*, 28, 1375-1388,
801 1994.
802

803 Rogge, W. F., Hildemann, L. M., Mazurek, M. A., Cass, G. R., Simoneit, B. R. T.: Sources of fine
804 organic aerosol. 2. Noncatalyst and catalyst-equipped automobiles and heavy-duty diesel trucks,
805 *Environ. Sci.Technol.*, 27, 636-651, 1993a.
806

807 Rogge, W. F., Mazurek, M. A., Hildemann, L. M., Cass, G. R., Simoneit, B. R. T.: Quantification of
808 urban organic aerosols at a molecular level: Identification, abundance and seasonal variation, *Atmos.*
809 *Environ.*, Part A., 27, 1309-1330, 1993b.

810 Ruehl, C. R., Nah, T., Isaacman, G., Worton, D. R., Chan, A. W. H., Kolesar, K. R., Cappa, C. D.,
811 Goldstein, A. H., and Wilson, K. R.: The Influence of molecular structure and aerosol phase on the
812 heterogeneous oxidation of normal and branched alkanes by OH, *J. Phys. Chem. A.*, 117, 3990-4000,
813 2013.

814

815 Schauer, J. J., Cass, G. R.: Source apportionment of wintertime gas-phase and particle-phase air
816 pollutants using organic compounds as tracers, *Environ. Sci. Technol.*, 34, 1821-1832, 2000.

817

818 Schauer, J. J., Rogge, W. F., Hildemann, L. M., Mazurek, M. A., Cass, G. R., Simoneit, B. R. T.:
819 Source apportionment of airborne particulate matter using organic compounds as tracers, *Atmos.*
820 *Environ.*, 30, 3837-3855, 1996.

821

822 Schmitter, J., Ignatiadis, I., Arpino, P.: Distribution of diaromatic nitrogen bases in crude oils,
823 *Geochimica et Cosmochimica Acta*, 47, 1975-1984, 1983.

824

825 Schwantes, R. H., Schilling, K. A., McVay, R. C., Lignell, H., Coggon, M. M., Zhang, X., Wennberg,
826 P. O., and Seinfeld, J. H.: Formation of highly oxygenated low-volatility products from cresol
827 oxidation, *Atmos. Chem. Phys.*, 17, 3453-3474, 2017.

828

829 Shakya, K. M., Griffin, R. J.: Secondary organic aerosol from photooxidation of polycyclic aromatic
830 hydrocarbons, *Environ. Sci. Technol.*, 44, 8134-8139, 2010.

831

832 Shen, R., Schäfer, K., Schnelle-Kreis, J., Shao, L., Norra, S., Kramar, U., Michalke, B., Abbaszade, G.,
833 Streibel, T., Zimmermann, R., Emeis, S.: Seasonal variability and source distribution of haze particles
834 from a continuous one-year study in Beijing, *Atmos. Pollut. Res.*, 9, 627-633, 2018.

835

836 Shen, G., Tao, S., Wei, S., Zhang, Y., Wang, R., Wang, B., Wei, L.I., Shen, H., Huang, Y., and Chen,
837 Y.: Emissions of parent, nitro, and oxygenated polycyclic aromatic hydrocarbons from residential
838 wood combustion in rural China, *Environ. Sci. Technol.*, 46, 8123-8130, 2012a.

839

840 Shen, G., Wei, S., Zhang, Y., Wang, R., Wang, B., Li, W., Shen, H., Huang, Y., Chen, Y., and Chen,
841 H.: Emission of oxygenated polycyclic aromatic hydrocarbons from biomass pellet burning in a
842 modern burner for cooking in China, *Atmos. Environ.*, 60, 234-237, 2012b.

843

844 Shen, G., Tao, S., Wang, W., Yang, Y., Ding, J., Xue, M., Min, Y., Zhu, C., Shen, H., and Li, W.:
845 Emission of oxygenated polycyclic aromatic hydrocarbons from indoor solid fuel combustion, *Environ.*
846 *Sci. Technol.*, 45, 3459-3465, 2011.

847

848 Simoneit, B. R. T., Kobayashi, M., Mochida, M., Kawamura, K., Lee, M., Lim, H.-J., Turpin, B. J.,
849 Komazaki, Y.: Composition and major sources of organic compounds of aerosol particulate matter
850 sampled during the ACE-Asia campaign, *J. Geophys. Res.: Atmospheres*, 109, D19S10,
851 doi:10.1029/2004JD004598, 2004.

852

853 Simoneit, B. R.: Biomass burning - a review of organic tracers for smoke from incomplete combustion,
854 *Appl. Geochem.*, 17, 129-162, 2002a.

855

856 Simoneit, B. R. T.: Biomass burning - a review of organic tracers for smoke from incomplete
857 combustion, *Appl. Geochem.*, 17, 129-162, 2002b.

858 Simoneit, B., Rogge, W., Lang, Q., Jaffé, R.: Molecular characterization of smoke from campfire
859 burning of pine wood (*Pinus elliottii*), *Chemosphere-Global Change Sci.*, 2, 107-122, 2000.
860

861 Simoneit, B. R. T., Sheng, G., Chen, X., Fu, J., Zhang, J., Xu, Y.: Molecular marker study of
862 extractable organic matter in aerosols from urban areas of China, *Atmos. Environ.*, 25, 2111-2129,
863 1991.
864

865 Simoneit, B. R.: Application of molecular marker analysis to vehicular exhaust for source
866 reconciliations, *Intl. J. Environ. Anal. Chem.*, 22, 203-232, 1985.
867

868 Simoneit, B. R. T.: Organic matter of the troposphere—III. Characterization and sources of petroleum
869 and pyrogenic residues in aerosols over the western united states, *Atmos. Environ.*, (1967) 18, 51-67,
870 1984.
871

872 Simoneit, B. R., Mazurek, M. A.: Organic matter of the troposphere-II. Natural background of biogenic
873 lipid matter in aerosols over the rural western united states, *Atmos. Environ.*, (1967) 16, 2139-2159,
874 1982.
875

876 Simoneit, B., Schnoes, H., Haug, P., Burlingame, A.: High-resolution mass spectrometry of
877 nitrogenous compounds of the Colorado Green River Formation oil shale, *Chem. Geol.*, 7, 123-141,
878 1971.
879

880 Simpson, C. D., Paulsen, M., Dills, R. L., Liu, L. J. S., Kalman, D. A.: Determination of
881 methoxyphenols in ambient atmospheric particulate matter: Tracers for wood combustion, *Environ.*,
882 *Sci. Technol.*, 39, 631-637, 2005.
883

884 Staples, C. A., Peterson, D. R., Parkerton, T. F., Adams, W. J.: The environmental fate of phthalate
885 esters: a literature review, *Chemosphere*, 35, 667-749, 1997.
886

887 Sun, Y., Wang, Z., Fu, P., Yang, T., Jiang, Q., Dong, H., Li, J., Jia, J.: Aerosol composition, sources
888 and processes during wintertime in Beijing, China, *Atmos. Chem. Phys.*, 13, 4577-4592, 2013.
889

890 Turpin, B. J., Lim, H.-J.: Species contributions to PM_{2.5} mass concentrations: Revisiting common
891 assumptions for estimating organic mass, *Aerosol Sci. Technol.*, 35, 602-610, 2001.
892

893 Wang, J., Ho, S. S. H., Huang, R., Gao, M., Liu, S., Zhao, S., Cao, J., Wang, G., Shen, Z., and Han, Y.:
894 Characterization of parent and oxygenated-polycyclic aromatic hydrocarbons (PAHs) in Xi'an, China
895 during heating period: An investigation of spatial distribution and transformation, *Chemosphere*, 159,
896 367, 2016.
897

898 Wang, W.: Regional distribution and air-soil exchange of polycyclic aromatic hydrocarbons (PAHs)
899 and their derivatives in Beijing-Tianjin area, Ph.D. Dissertation, Peking University, Beijing, China,
900 2010.
901

902 Wang, G., Kawamura, K., Lee, S., Ho, K., Cao, J.: Molecular, seasonal, and spatial distributions of
903 organic aerosols from fourteen Chinese cities, *Environ. Sci. Technol.*, 40, 4619-4625, 2006.
904

905 Wang, G., Kawamura, K.: Molecular characteristics of urban organic aerosols from Nanjing: A case
906 study of a mega-city in China, *Environ. Sci. Technol.*, 39, 7430-7438, 2005.
907

908 Wang, Z., Bi, X., Sheng, G., Fu, J.: Characterization of organic compounds and molecular tracers from
909 biomass burning smoke in South China I: Broad-leaf trees and shrubs, *Atmos. Environ.*, 43, 3096-
910 3102, 2009.
911

912 Wei, S., Huang, B., Liu, M., Bi, X., Ren, Z., Sheng, G., and Fu, J.: Characterization of PM_{2.5}-bound
913 nitrated and oxygenated PAHs in two industrial sites of South China, *Atmos. Res.*, 109, 76-83, 2012.
914

915 Welthagen, W., Schnelle-Kreis, J., Zimmermann, R.: Search criteria and rules for comprehensive two-
916 dimensional gas chromatography–time-of-flight mass spectrometry analysis of airborne particulate
917 matter, *J. Chromatogr., A* 1019, 233-249, 2003.
918

919 Wu, X., Vu, T. V., Shi, Z., Harrison, R. M., Liu, D., Cen, K.: Characterization and Source
920 Apportionment of Carbonaceous PM_{2.5} Particles in China - A Review, *Atmos. Environ.*, 189, 187-212,
921 2018.
922

923 Yao, L., Yang, L., Yuan, Q., Yan, C., Dong, C., Meng, C., Sui, X., Yang, F., Lu, Y., Wang, W.:
924 Sources apportionment of PM_{2.5} in a background site in the North China Plain, *Sci. Tot. Environ.*,
925 541, 590-598, 2016.
926

927 Yee, L. D., Kautzman, K. E., Loza, C. L., Schilling, K. A., Coggon, M. M., Chhabra, P. S., Chan, M.
928 N., Chan, A. W. H., Hersey, S. P., Crouse, J. D., Wennberg, P. O., Flagan, R. C., Seinfeld, J. H.:
929 Secondary organic aerosol formation from biomass burning intermediates: phenol and
930 methoxyphenols, *Atmos. Chem. Phys.*, 13, 8019-8043, 2013.
931

932 Zhang, H., Worton, D. R., Shen, S., Nah, T., Isaacman-VanWertz, G., Wilson, K. R., and Goldstein, A.
933 H.: Fundamental time scales governing organic aerosol multiphase partitioning and oxidative aging,
934 *Environ. Sci. Technol.*, 49, 9768-9777, 2015.
935

936 Zhang, Y.-X., Shao, M., Zhang, Y.-h., Zeng, L.-M., He, L.-Y., Zhu, B., Wei, Y., Zhu, X.: Source
937 profiles of particulate organic matters emitted from cereal straw burnings, *J. Environ. Sci.*, 19, 167-175,
938 2007.
939

940 Zhang, Q., Anastasio, C., Jimenez-Cruz, M.: Water-soluble organic nitrogen in atmospheric fine
941 particles (PM_{2.5}) from northern California, *J. Geophys. Res.: Atmospheres*, 107, D11, 4112,
942 10.1029/2001JD000870, 2002.
943

944 Zhao, J., Peng, P. A., Song, J., Ma, S., Sheng, G., Fu, J.: Characterization of organic matter in total
945 suspended particles by thermodesorption and pyrolysis-gas chromatography-mass spectrometry,
946 *J. Environ. Sci.*, 21, 1658-1666, 2009.
947

948 Zhou, J., Wang, T., Zhang, Y., Zhong, N., Medeiros, P. M., Simoneit, B. R. T.: Composition and
949 sources of organic matter in atmospheric PM₁₀ over a two year period in Beijing, China, *Atmos. Res.*,
950 93, 849-861, 2009.
951

952 **TABLE LEGENDS:**

953

954 **Table 1:** Comparison of identified organic compounds with earlier studies in Beijing. Data from the
955 present study are mean \pm s.d. for n = 33 samples.

956

957 **Table 2:** Molecular formula, diagnostic ions and average concentrations of hopanes identified in
958 PM_{2.5}.

959

960 **Table 3:** Estimated average concentrations of unknown compounds (ng m⁻³) in each section of the
961 chromatogram for haze and non-haze conditions.

962

963

964 **FIGURE LEGENDS:**

965

966 **Figure 1:** The percentages of the organic compound groups in the total identified organic compounds.

967

968 **Figure 2:** A comparison of organic compound groups between non-haze and haze days. The average
969 total concentration of the identified group was calculated in the non-haze (13 days) and
970 haze periods (20 days), respectively.

971

972 **Figure 3:** The distribution of concentrations of PAHs (shaded bars, 25%-first quartile, 75%-third
973 quartile).

974

975 **Figure 4:** The molecular distributions of aliphatic hydrocarbons and other homologous series,
976 including n-alkanes, branched alkanes, n-alkenes, carbonyl compounds (n-alkanals, n-alkan-
977 2-ones, n-alkan-3-ones), n-alkanoic acid and alkanols on haze and non-haze days.

978

979 **Figure 5:** The molecular distributions of n-C_n-cyclohexane, alkyl-bicyclic-alkanes, alkyl-benzenes, n-
980 C_n-benzenes, alkyl-furanones and alkyl-pyridines on haze and non-haze days.

981

982 **Figure 6:** The concentration (ng m⁻³) sum of identified and unknown organic compounds in each
983 chromatogram image section during (a) non-haze and (b) haze days.

984

985
986

Table 1: Comparison of identified organic compounds with earlier studies in Beijing. Data from the present study are mean \pm s.d. for n = 33 samples.

Compound name	Concentrations, ng m ⁻³	
	Present	Previous study
n-alkanols		
1-Dodecanol	2.27 \pm 1.49	0.90 j;
1-Tetradecanol	24.2 \pm 88.9	3.00 j;
1-Hexadecanol	6.66 \pm 20.7	1.2 d; 6.30 j;
1-Octadecanol	1.69 \pm 1.65	3.1 d; 20.1 j;
1-Eicosanol	3.71 \pm 2.96	19.5 j;
n-alkanoic acids		
Hexanoic acid	1.80 \pm 1.54	30.4 i; 0.00 j;
Heptanoic acid	0.73 \pm 1.05	0.62 j;
Octanoic acid	2.97 \pm 2.56	29.6 i; 0.62 j;
Nonanoic acid	1.23 \pm 1.37	2.07 j;
Decanoic acid	22.8 \pm 25.2	6.4 d; 5.8 i; 1.24 j;
Hopanes		
18 α (H)22,29,30-trisnorhopane	2.91 \pm 3.06	0.22 j;
17 α (H)-22,29,30-Trisnorhopane	1.56 \pm 2.74	2.75 a; 2.3 d; 0.5 i; 0.21 j;
17 α (H)21 β (H)-30-norhopane	9.92 \pm 7.63	7.19 a; 4.1 d;
17 β (H)21 α (H)-hopane(moretane)	5.77 \pm 6.12	1.32 j; 1.9 d;
17 α (H)21 β (H)-hopane	3.71 \pm 5.49	3.51 a; 3.2 d; 0.8 i; 1.54 j;
17 α (H)21 β (H)-homohopane(22R)	1.32 \pm 1.31	0.63 a; 1.2 d; 0.42 j;
17 α (H)21 β (H)-homohopane(22S)	0.83 \pm 0.93	2.94 a; 1.2 d; 0.63 j;
17 α (H),21 β (H)-bishomohopane(22S)	5.23 \pm 6.51	0.7 d;
17 α (H)21 β (H)-bishomohopane(22R)	1.41 \pm 1.73	0.7 d;
Subtotal	32.7\pm24.7	
PAHs		
Naphthalene (NAP,2-rings)	6.03 \pm 4.52	0.22 b; 2.4 i;
Acenaphthylene (ACY, 2-rings)	12.7 \pm 9.93	0.065 b; 0.3 i;
Acenaphthene (ACE, 2-rings)	6.04 \pm 8.94	0.79 b; 0.51g; 0.3 i;
Fluorene (FLU, 3-rings)	16.6 \pm 13.0	1.18 b; 1.65g; 0.5 i; 15.6 j;
Phenanthrene (PHE, 3-rings)	8.59 \pm 8.49	14.0 b; 0.9 d; 1.1 e; 21.65 f; 30.3g; 0.9 i; 95.7 j;
Anthracene (ANT, 3-rings)	6.14 \pm 6.53	1.70 b; 3.3 d; 5.74g; 0.2 i; 52.3 j;
Pyrene (PYR, 4-rings)	18.9 \pm 18.2	22.3 b; 12 d; 0.58 e; 31.3 f; 64.4g; 1.0 i; 235 j;
Fluoranthene (FLT, 4-rings)	21.0 \pm 20.4	41.5 b; 11 d; 0.23 e; 31.8 f; 76.4g; 1.1 i; 222 j;
Chrysene (CHR, 4-rings)	25.5 \pm 19.3	21.8 b; 1.00 d; 1.00 e; 50.6 f; 62.7g; 1.3 i; 140 j;
Benz[a]anthracene (BaA, 4-rings)	17.6 \pm 14.6	23.5 b; 19 d; 43.4 f; 45.1g; 0.8 i; 62.9 j;
Benzo[k]fluoranthene (BkF, 4-rings)	8.81 \pm 7.68	17.0 b; 8.3 d; 33.6g; 0.7 i; 30.5 j;
Cyclopenta[cd]pyrene (CcP, 5-rings)	8.60 \pm 10.2	68.0 j;
Perylene (PER, 5-rings)	3.20 \pm 2.69	2.81 b; 14 d; 5.99g; 0.2 i;

Compound name	Concentrations, ng m ⁻³	
	Present	Previous study
Benzo[b]fluoranthene (BbF, 5-rings)	38.5±31.8	34.0 b; 59 d; 33.1 f; 53.6g; 2.3 i; 134 j;
Benzo[a]pyrene (BaP, 5-rings)	13.1±13.8	14.6 b; 14 d; 0.08 e; 40.2 f; 28.6g; 1.1 i; 41.3 j;
Indeno[1,2,3-cd]pyrene (IcdP, 6-rings)	12.3±8.82	18.1 b; 15.2 d; 0.32 e; 40.9 f; 32.3g; 1.2 i; 18.2 j;
Benzo[ghi]perylene (BghiP, 6-rings)	12.4±11.1	12.2 b; 12 d; 0.33 e; 22.2g; 2.6 i; 59.0 j;
Benzo[e]pyrene (BeP, 5-rings)	15.4±10.3	12.4 b; 12 d; 0.65 e; 24.7g; 1.3 i; 72.6 j;
Dibenzo [a,h]pyrene (DBA, 5-rings)	5.68±7.35	2.01 b; 3.1 d;
Benzo[ghi]fluoranthene (BghiF,5-rings)	15.1±15.8	0.08 e; 15.3 f;
O-PAHs		
Anthracenedione (AQ)	5.12±5.97	108 b;
7,12-Benz[a]anthracenequinone (BaAQ)	4.09±3.61	2.14 b;
Aceanthrenequinone (AceAntQ)	2.41±2.89	0.01b;
Phenanthraquinone (PQ)	1.45±1.08	0.13 b;
9-Fluorenone (9-FluQ)	3.78±4.01	28.3g;
Alkylated-(PAHs & OPAHs)		
Pyrene, 1-methyl- (1-MePYR)	21.5±21.5	3.80 b
Phenanthrene, 1-methyl- (1-MePHE)	5.29±5.38	4.29 b
Retene	5.39±9.72	0.12 e; 0.5 i;
Ester		
Dibutyl phthalate (DBP)	16.9±15.5	21 d; 3.00 j;
Diethyl Phthalate (DEP)	2.67±2.91	3.5 d; 24.0 j;
Di(2-ethylhexyl)-phthalate (DEHP)	16.0±12.6	130 d;
Diisobutyl phthalate	49.7±43.2	22 d;
Dimethyl phthalate	2.58±2.80	1.5 d;
Biomarkers		
Levoglucosan	355±232	310 a; 790.3 c; 171 d; 78 h; 97.1 i; 830 j;
Phytone	14.7±11.7	0.9 j;
Phytane	1.94±1.05	2.3 i; 1.30 j;
Pristane	2.24±1.69	1.8 i; 0.67 j;
Other nitrogen compounds (Nitro, amine, heterocyclic compounds)		
Benzo[f]quinoline	4.40±4.66	3.10 j;
Isoquinoline	0.80±0.83	0.22 j;
Phenolic compounds		
1-Naphthalenol (1-OH-NAP)	1.56±5.61	0.22 b
2-Naphthalenol (2-OH-NAP)	1.15±1.21	2.74 b
2-Dibenzofuranol (2-OHDBF)	1.84±2.09	1.47 b

- 987 a. Beijing, PKU, Heating seasons (Ma et al., 2018);
988 b. Beijing, PKU, Heating seasons (Lin et al., 2015);
989 c. Beijing, China University of Geosciences (Beijing), winter (Shen et al., 2018);
990 d. Beijing, winter of 2003 (Wang et al., 2006)

- 991 e. Beijing, urban, June (Simoneit et al., 1991);
- 992 f. Beijing, urban, haze period (Gao et al., 2016);
- 993 g. Beijing, PKU, haze period (Li et al., 2019);
- 994 h. Beijing, PKU, winter (He et al., 2006b)
- 995 i. During the 2008 Beijing Olympic Games, PKU sites, (Guo et al., 2013);
- 996 j. Beijing, urban, winter (Zhou et al., 2009);
- 997
- 998

999
1000
1001

Table 2: Molecular formula, diagnostic ions and average concentrations of hopanes identified in PM_{2.5}.

Compounds		Molecular formula	Diagnostic ions	IAP, ng m ⁻³
18 α (H)22,29,30-trisnorneohopane	Ts	C ₂₇ H ₄₆	191/370	2.91 \pm 3.06
17 α (H)-22,29,30-Trisnorhopane	Tm	C ₂₇ H ₄₆	191/370	1.56 \pm 2.74
17 α (H)21 β (H)-30-norhopane	29 $\alpha\beta$	C ₂₉ H ₅₀	191/398	9.92 \pm 7.63
17 β (H)21 α (H)-hopane(moretane)	30 $\beta\alpha$	C ₃₀ H ₅₂	191/412	5.77 \pm 6.12
17 α (H)21 β (H)-hopane	30 $\alpha\beta$	C ₃₀ H ₅₂	191/412	3.71 \pm 5.49
17 α (H)21 β (H)-homohopane(22R)	30 $\alpha\beta$ -22R	C ₃₁ H ₅₄	191/426	1.32 \pm 1.31
17 α (H)21 β (H)-homohopane(22S)	30 $\alpha\beta$ -22S	C ₃₁ H ₅₄	191/426	0.83 \pm 0.93
17 α (H),21 β (H)-bishomohopane(22S)	30 $\alpha\beta$ -22S	C ₃₂ H ₅₆	191/440	5.23 \pm 6.51
17 α (H)21 β (H)-bishomohopane(22R)	30 $\alpha\beta$ -22R	C ₃₂ H ₅₆	191/440	1.41 \pm 1.73

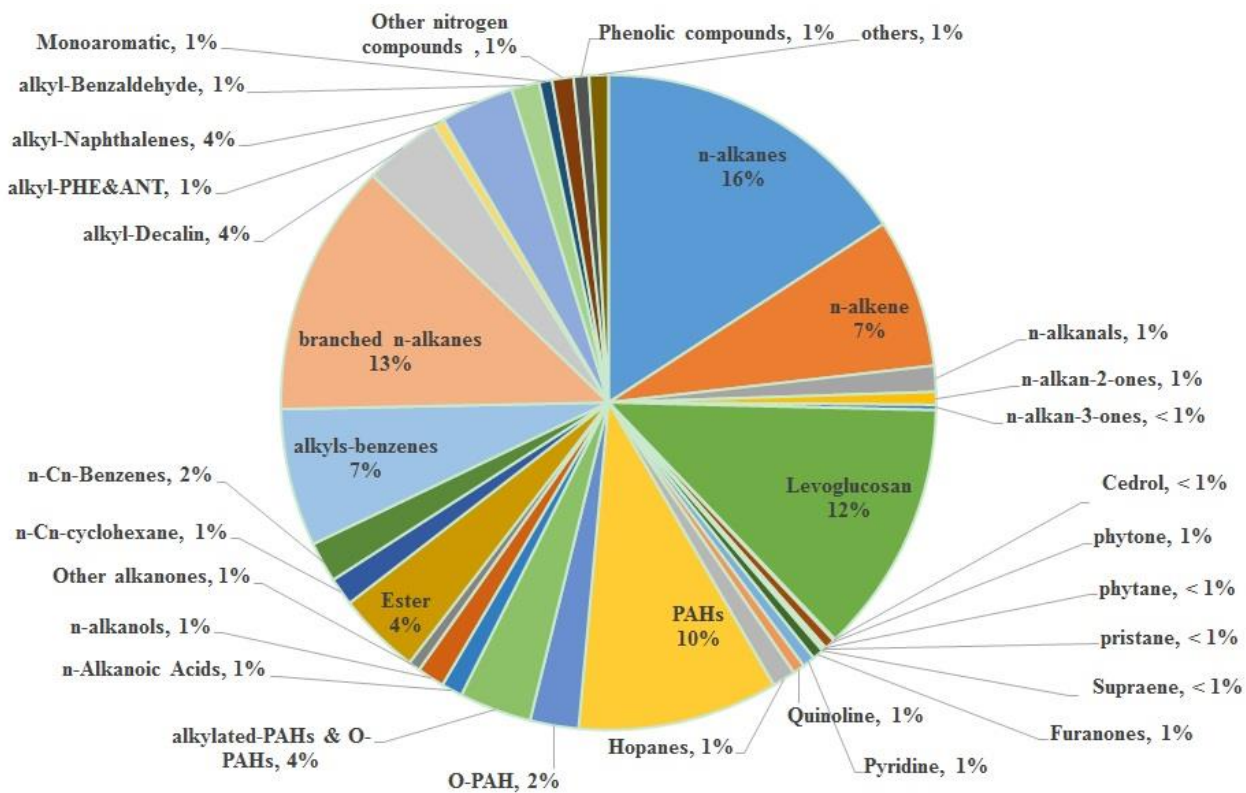
1002

1003
1004
1005

Table 3: Estimated average concentrations of unknown compounds (ng m^{-3}) in each section of the chromatogram for haze and non-haze conditions.

Section	Characteristics of organic compounds	Non-haze		Haze	
		Total	Unidentified	Total	Unidentified
1	Low molecular weight: ➤ carbon numbers (n-alkanes) ≤ 17 ; ➤ monoaromatics;	802	546	911	632
2	Medium molecular weight: ➤ $17 < \text{carbon numbers (n-alkanes)} \leq 23$; ➤ Oxidized hydrocarbons (alkanals, alkanones);	334	137	483	147
3	Medium molecular weight: ➤ $23 < \text{carbon numbers (n-alkanes)} \leq 27$; ➤ Oxidized hydrocarbons (alkanals, alkanones);	573	215	1060	228
4	High molecular weight: ➤ carbon numbers (n-alkanes) ≥ 27 ;	351	188	730	320
5	Oxidized monoaromatics;	621	289	1309	985
6	2 rings PAHs	485	303	1556	879
7	3-6 rings PAHs and hopanes;	792	440	1337	774
Total		3958	2119	7385	3964

1006



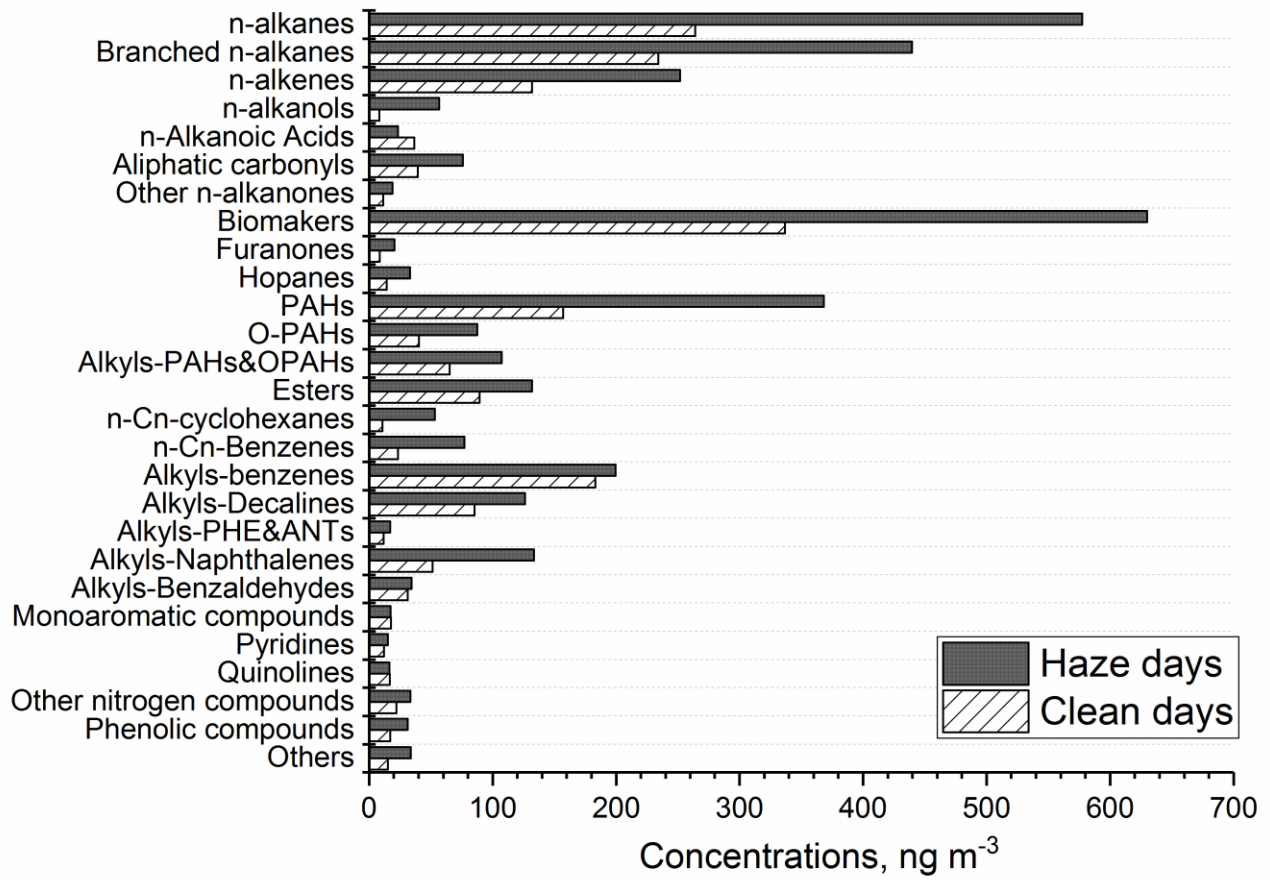
1007

1008

1009

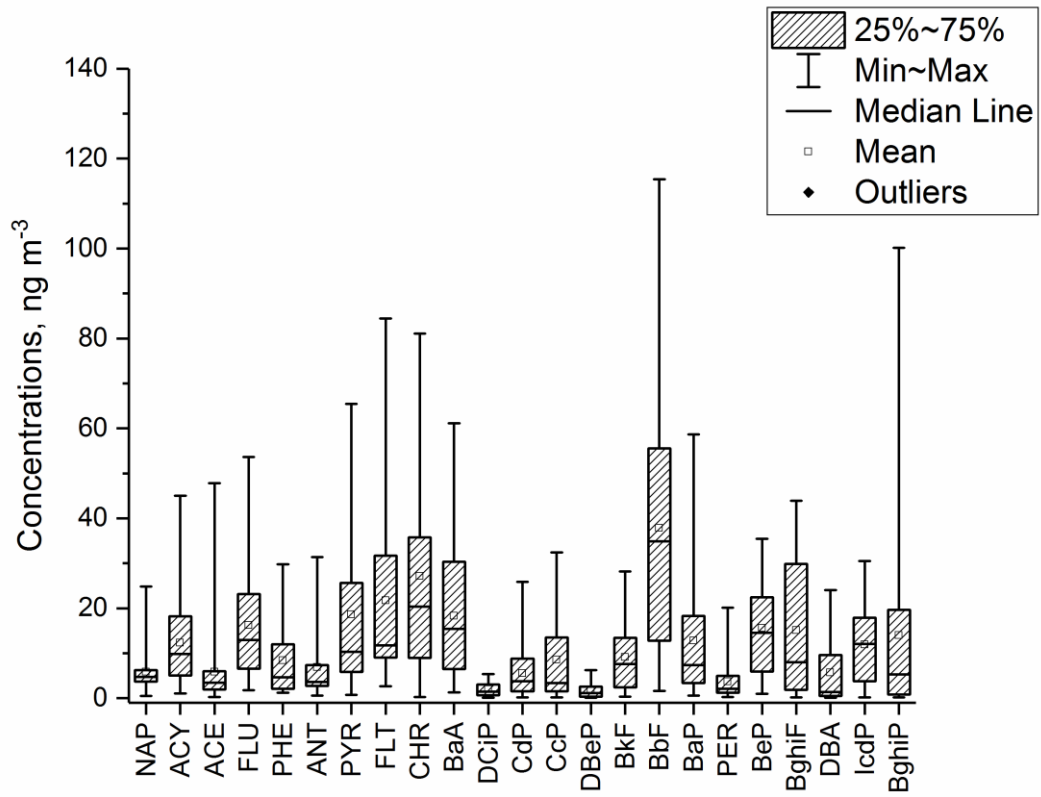
Figure 1: The percentages of the organic compound groups in the total identified organic compounds.

1010



1011

1012 **Figure 2:** A comparison of organic compound groups between non-haze and haze days. The average
1013 total concentration of the identified group was calculated in the non-haze (13 days) and haze periods
1014 (20 days), respectively.
1015

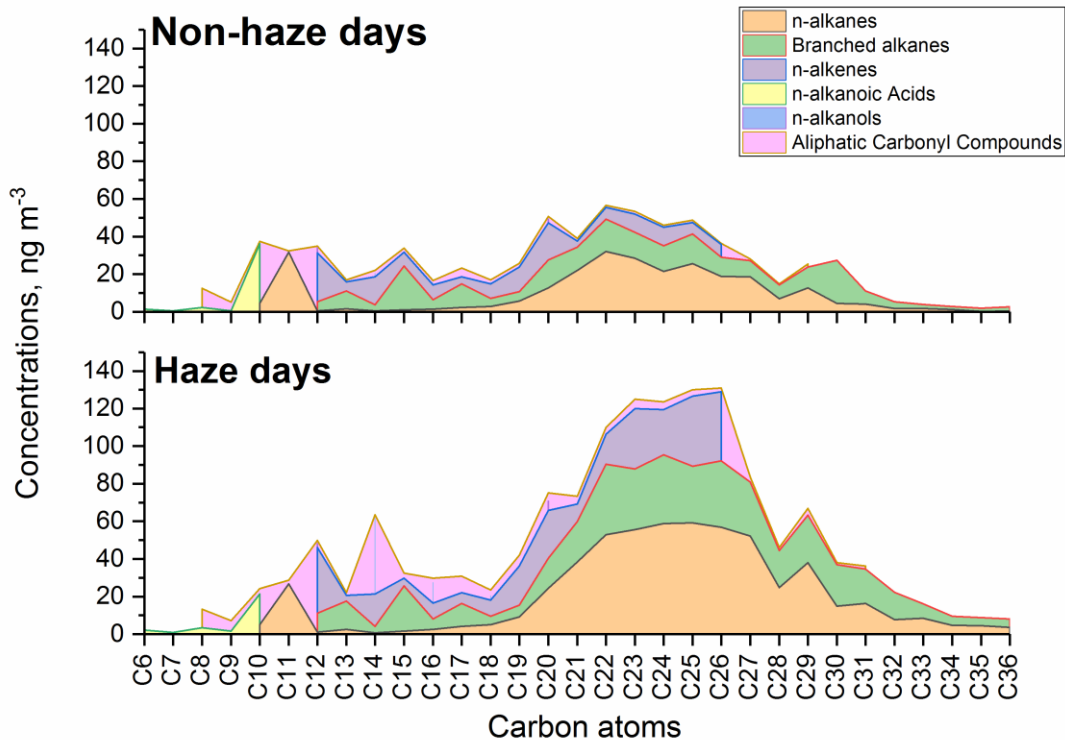


1016

1017 **Figure 3:** The distribution of concentrations of PAHs (shaded bars, 25%-first quartile, 75%-third
 1018 quartile).

1019

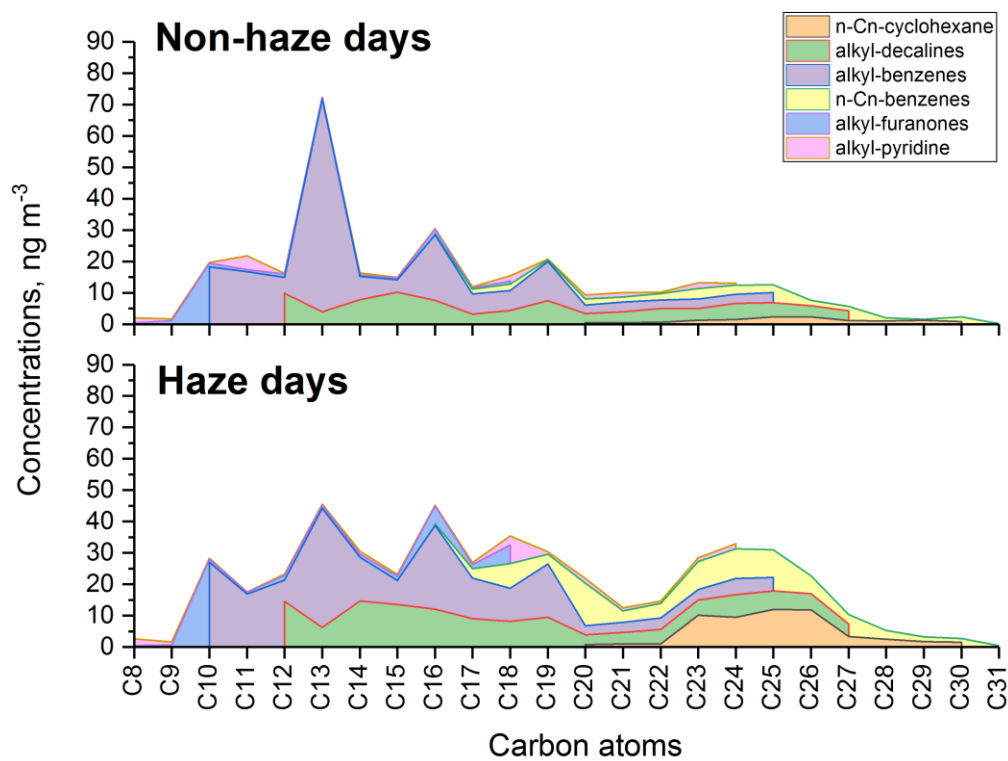
1020



1021

1022 **Figure 4:** The molecular distributions of aliphatic hydrocarbons and other homologous series, including
 1023 n-alkanes, branched alkanes, n-alkenes, carbonyl compounds (n-alkanals, n-alkan-2-ones, n-alkan-3-
 1024 ones), n-alkanoic acid and alkanols on haze and non-haze days.

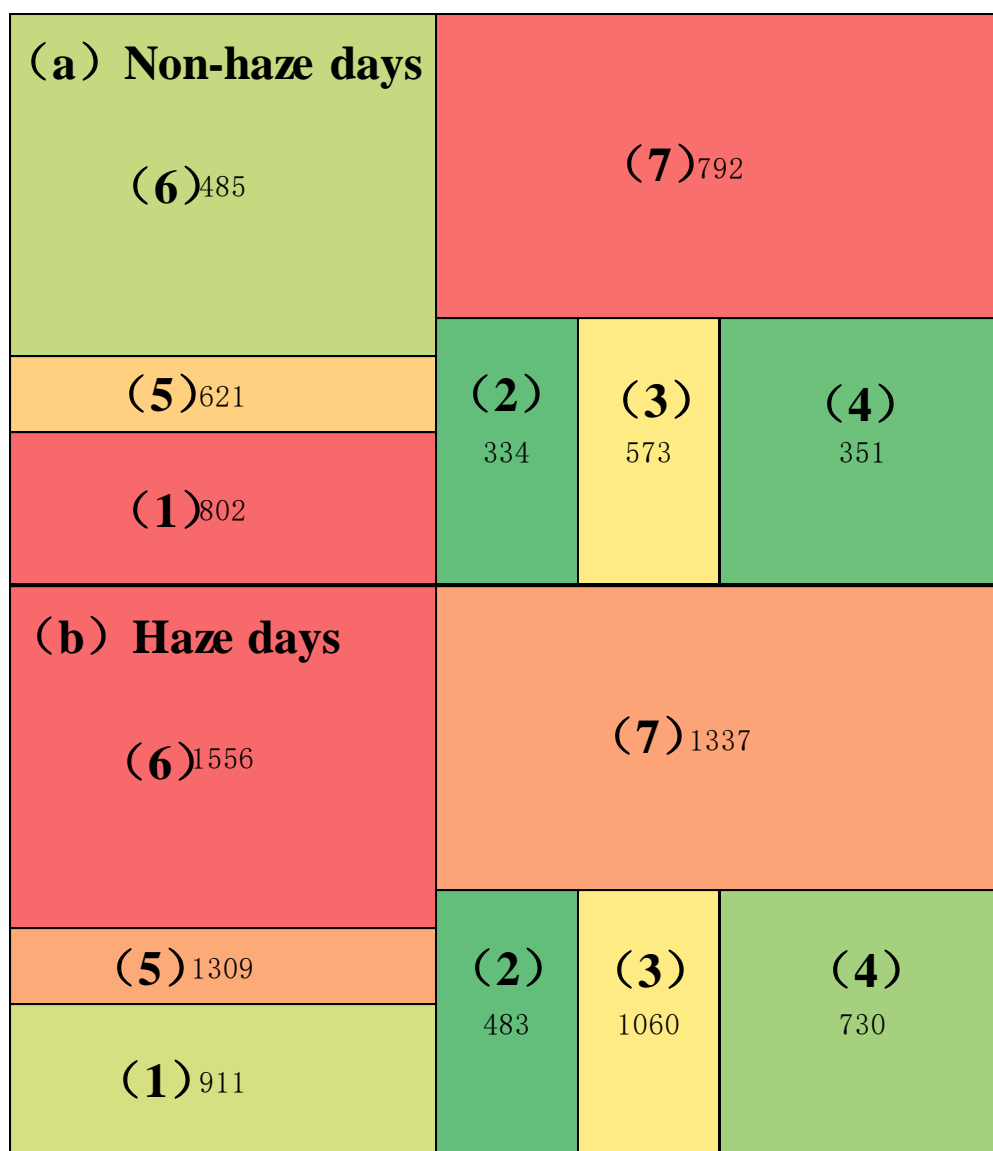
1025



1027

1028 **Figure 5:** The molecular distributions of n-C_n-cyclohexane, alkyl-bicyclic-alkanes, alkyl-benzenes, n-
 1029 C_n-benzenes, alkyl-furanones and alkyl-pyridines on haze and non-haze days.

1030



1031

1032

1033

1034

1035

1036

Figure 6: The concentration (ng m⁻³) sum of identified and unknown organic compounds in each chromatogram image section during (a) non-haze and (b) haze days.